8-2016

A Dose Distribution Study of Uranyl Nitrate in Zebrafish using Liquid Scintillation and Passivated Implanted Planar Silicon Detectors

Lee A. Alleman
Purdue University

PURDUE UNIVERSITY
GRADUATE SCHOOL
Thesis/Dissertation Acceptance

This is to certify that the thesis/dissertation prepared

By Lee Armond Alleman

Entitled

A DOSE DISTRIBUTION STUDY OF URANYL NITRATE IN ZEBRAFISH USING LIQUID SCINTILLATION AND PASSIVATED IMPLANTED PLANAR SILICON DETECTOR

For the degree of Master of Science

Is approved by the final examining committee:

Huiling L. Nie
Chair

James Schweitzer
Co-chair

Jennifer L. Freeman
Co-chair

To the best of my knowledge and as understood by the student in the Thesis/Dissertation Agreement, Publication Delay, and Certification Disclaimer (Graduate School Form 32), this thesis/dissertation adheres to the provisions of Purdue University's "Policy of Integrity in Research" and the use of copyright material.

Approved by Major Professor(s): Huiling L. Nie

Approved by: Shuang Lui 7/1/2016

Head of the Departmental Graduate Program Date

A DOSE DISTRIBUTION STUDY OF URANYL NITRATE IN ZEBRAFISH USING LIQUID SCINTILLATION AND PASSIVATED IMPLANTED PLANAR SILICON DETECTOR

A Thesis

Submitted to the Faculty

of

Purdue University

by

Lee A. Alleman

In Partial Fulfillment of the

Requirements for the Degree

of

Master of Science

August 2016

Purdue University

West Lafayette, Indiana

This work is dedicated to my family:

We have lived in numerous cities over the years,

Have had numerous friends that come and go,

And even during those times I spend long periods away,

They will always be HOME for me.

ACKNOWLEDGEMENTS

I would like to acknowledge my thesis committee members for their guidance and advice in turning a research project into a thesis:

Dr. Linda Nie (Chair)

Dr. Jim Schweitzer (Co-Chair)

Dr. Jennifer Freeman (Co-Chair)

I would also like to thank Dr. Linda Nie as my advisor for her tireless commitment and dedication to my success here at Purdue; and Dr. Jim Schweitzer for his support and advice in my research and this thesis.

Members of the lab provided a tremendous amount of assistance with all my questions and concerns. Thank you Katharine Horzmann

Heather, Michael, and Olivia: you three supported me for the last two years.

k you

Disclaimer: The views expressed in this article are those of the author and do not necessarily reflect the official policy or position of the Department of the Navy, Department of Defense, or the United States Government. The author is a military service member. This work was prepared as part of the author's official duties. Title 17, USC, §105 provides that 'Copyright protection under this title is not available for any work of the U.S. Government.' Title 17, USC, §101 defines a U.S. Government work as a work prepared by a military service member or employee of the U.S. Government as part of that person's official duties."

TABLE OF CONTENTS

Page

LIST OF TABLES

LIST OF FIGURES

ABSTRACT

Alleman, Lee A. M.S., Purdue University, August 2016. A Dose Distribution Study of Uranyl Nitrate in Zebrafish using Liquid Scintillation and Passivated Implanted Planar Silicon Detectors. Major Professor: Linda H. Nie.

Standard curves for a Perkin Elmer TriCarb 2800 liquid scintillation detector (LSC) and a Ludlum 3030p Passivated Implanted Planar Silicon detector have been developed and utilized for studying the dose distribution of depleted uranium (DU) within zebrafish. The DU source was crystallized uranyl nitrate ($N_2O_8U•6H_2O$) solution, normally used for staining in electron microscopy with a manufactured average specific activity of 0.3 uCi/g. Zebrafish ,both larvae and adults, were exposed to three different mass concentrations, dissected, dissolved and counted using an LSC. The counts were compared to the standard curve correlating the measured activity to that of the mass absorbed. It was found that the larvae were more tolerant to the toxicity of the DU by almost a factor of 10 showing survival up to 200 ppm where the adults had zero survival when exposed to concentrations above 20 ppm. The absorbed DU was observed to concentrate more heavily in the skeletal structure and the blood containing organs (liver and heart) when comparing the relative mass concentrations observed in each organ compared to that of the whole fish exposed to the same concentration. The highest absorbed dose rate was found in the skeletal system at 3.5 mGy/d followed by the blood containing organs at 2.2 mGy/d when exposed to 20 ppm DU. It was also noted that the bioconcentration factors (BCF) of the adult zebrafish followed the same trend observed in similar studies. As the mass concentration of DU was lowered, the BCF calculated for fish exposed increased with a BCF of 130.6 found for those exposed to 20 ppm U and a BCF of 774.2 for fish exposed to 2 ppm. This method shows to present a suitable way of

developing a dose distribution for DU along with similar isotopes which will be instrumental in studying the long term effects of more specific exposures to natural radioactive metals combined with other common environmental exposures.

CHAPTER 1. INTRODUCTION

1.1 Radiation Biology and Charged Particle Effects

The increased use of charged particle radiation in many types of therapy along with growing concerns of natural exposure warrants extensive studies on the long term biological effects and distribution of such particle emitters. Charged particle therapy has proven to be an effective method of treating certain conditions as it provides a much higher liner energy transfer than photons with a much higher relative biological effectiveness (RBE). Unfortunately, due to the variety of ranges of the RBE, it is vital that targeting methods are extremely accurate as any dose deposited outside of the targeted area will see significant damage. Some of these charged particles, such as alphas, are also part of our everyday exposure. Natural elements include radioactive isotopes that decay over time emitting alpha radiation. Although the emission is fairly small, it is important to understand the distribution of some of these isotopes and relate how they may or may not affect human health, specifically combined with exposure from other toxic elements.

In studying human or animal dose distributions, it is important to understand the biological effects to cells and tissues that ionizing radiation may cause. To properly

categorize these effects, a discussion on some of the important physical, biological, and chemical changes that occur due to radiation is in order.

An explanation of how damaging ionizing radiation can be to cells is defined mostly by two terms: linear energy transfer and radiation biological effectiveness The linear energy transfer (LET) of a type of radiation is basically the average energy transferred per unit path length as it passes through a given medium, typically represented with units of $keV/\mu m$. Particles of higher mass or charge typically have higher LETs, for example, the LET of an alpha particle from uranium decay is approximately 80 times higher than that of a 250 kV x-ray. To better relate different types of radiation and the effects they have on cells, you can correlate the RBE of different isotopes. RBE uses the ratio in absorbed dose of 250 kV x-rays to that of a test radiation's ability to kill a population of cell s. The LET and RBE of a radiation is used to determine its radiation weighting factor, W_R (Hall EJ & Giaccia AJ 2012).

Most cells come equipped with the ability to repair damage caused by ionizing radiation. The most damaging course for ionizing radiation is its effects on the DNA. The two major occurrences to DNA is that the DNA can be damaged directly from the ionizing radiation or indirectly by the production of free radicals that tend to chemically damage the DNA. Direct DNA damage can occur when a charged particle directly interacts with the strands of DNA and separates them from their base. This is the primary mode of DNA damage by alpha and beta radiation. Indirect damage occurs when the ionizing radiation electrostatically interacts with a a nearby molecule which ionizes it and results in radiolytic decomposition of the molecule The free radicals that are then produced go on to disrupt the operation of the DNA itself.

There are multiple results that can occur when a cell is affected by ionizing radiation. A single strand break typically occurs when one side of the helix is damaged. Since human DNA consists of a double helix, the damage to one is easily repaired because the cell has the ability to use its replicate on the other side. If a break occurs in both strands of the DNA relatively close to each other, the resulting repair could end up in the wrong configuration which typically results in the DNA being able to return to its original state. Double strand breaks of DNA typically lead to cell death, mutation, or carcinogenesis (Hall EJ & Giaccia AJ 2012).In clonogenic survival, the cell will repair itself and act and reproduce normally. Normal reproduction is typically defined by the cells ability to produce 50 daughter cells following repair. If the cell is unable to repair the damage it may die via apoptosis or reproductive death. Apoptosis is a common occurrence in white blood cells when exposed to ionizing radiation where the cell function ceases immediately following (Wilkins RC et al. 2001). This is why it is so important to get lymphocyte readings of an individual following radiation exposure as the immune system is the first to fail. Granted the damage isn't too significant, the cell is able to function normally until mitosis.

Chromosomal aberrations can occur during these breaks which can stop the cell from dividing successfully thus resulting in cell death. Without direct observation of the aberrations, the cell can appear to function normally as the abnormality may not occur on the first division. Because of the nature of cell repair and division, successful clonogenic survival is concluded after 50 daughters are produced. If the cell incorrectly repairs itself, it could become mutated and form cancerous cells. Hanahan and Weinberg state:

> "Cancerous cells are changed such that they produce self-sufficient growth patterns, have an insensitivity to anti-growth signals, can invade other tissues and metastasize, exhibit limitless replicative potential (immortal), have sustained angiogenesis, and evade apoptosis; these conditions are the hallmarks of cancer "(Hanahan D and Weinberg RA 2000).

The basic characteristics of the cell exposed to ionizing radiation determine its sensitivity. The Law of Bergonie and Tribondeau states cells are most radiosensitive if they have a greater reproductive activity, a long dividing life, and are unspecified (such as stem cells) (Bergonie J and Triboneau L 1906; translated and republished in 1956). This is why fetuses and children are considered more sensitive to radiation and thus have much lower limits when compared to adults. Different tissue types follow this rule also, for example, blood cells in the bone or more susceptible to radiation than the bone surfaces. This is defined in ICRP 103, with revised tissue weighting factors (W_t) denoting the different sensitivities of different tissues in the human body.

1.2 Use of Zebrafish (*Danio rerio*)

The zebrafish has become one of the preferred vertebrate model systems in biomedical research. Several features make the zebrafish a unique vertebrate model for toxicological studies including: the short generation time, high fertility, external fertilization, *ex utero* embryonic development, transparent embryos, small size of adult organism, a short life span, and relatively low-costs associated with maintenance (Brennan 2014). In this study we are studying the dose distribution from depleted uranium (DU) at levels comparable to environmental exposure. This will allow future

studies of genetic and epigenetic mechanisms of a developmental heavy metal exposure combined with radiation exposure that is representative of environmental exposures to the human population.

There are many benefits to using zebrafish for an experiment such as this as an alternative to mammalian species. It is very important to reduce animal suffering when used in research, and this is usually accomplished by using the least sentient organism possible to answer the question. Zebrafish have similar genetics to that of humans, most importantly, as vertebrates, they possess a higher similar sequence and homology to other mammals, including humans (Howe K. et al, Nature 2014). Due to the embryos and larvae being transparent, it's also possible to reduce animal suffering by using non-invasive imaging techniques to observe the impact of genetic or chemical manipulation.

Maintaining zebrafish colonies is cost effective and due to their small size and simple nature, it's easier to keep them in similar environments and conditions that would simulate a natural habitat. These factors minimize housing stress and the impact it may have on experimental outcomes which reduces the number of animals that may be needed due to variations that can be caused by stress.

Zebrafish also have the benefit of a large amount of offspring which ensures a steady supply of animals for research. When compared to rodents, which have 5-10 offspring per pairing, zebrafish can produce anywhere from 100 to 400 per pair . For this experiment, it wasn't clear what effects the DU would have on the fish themselves. To achieve an adequate count rate from absorbed DU, the amount needed to be added to their environment ranged from 10 to 1000 ppm. Being able to quickly replace fish lost

while figuring out the lethality of DU was instrumental in collecting the data required to calculate the distribution within the body.

1.3 Alpha and Beta Production

1.3.1 Alpha Production

Alpha decay is the emission of an alpha particle, which is the nucleus of $^{4}_{2}He$, from the nucleus. The helium nucleus is very stable and leaves the parent nucleus minus two protons and 2 neutrons. For example:

$$^{238}_{92}U \rightarrow {}^{234}_{90}Th + {}^{4}_{2}He + Q_{\alpha}$$

Both the mass number and the atomic number are conserved in the reaction. The mass number of 238 on the left side is equal to the mass number of 234 and 4 on the right, same with the atomic number. The decay mechanism depends on two protons from the highest energy levels and two neutrons from its highest energy levels combine to form the alpha particle inside the nucleus, also known as a “quasi-bound-state” .

The Q_{α}-value of the decay is the difference in the mass between the parent nuclide and that of the daughter and the alpha combined, multiplied by the speed of light squared. It is also equal to the difference between the sum of the binding energies of the parent nucleus and the daughter and the alpha particle.

$$Q_{\alpha} = (m_p - m_d - m_{\alpha})c^2$$

$$Q_{\alpha} = T_{\alpha} + T_D$$

The total coulomb energy of the nucleus is lowered by the emission of the alpha particle. This raises the stability of the heavy nuclide but has no effect on the binding energy per nucleon. As a result, the tightly bound alpha particle has almost the same

binding energy as the nucleus per nucleon. One main feature of alpha decay is that the energy of the alpha particles generally rises with the parent's atomic number but the kinetic energy of the emitted particle is less than the coulomb barrier in the reverse reaction between the daughter nucleus and the alpha (Turner 2012). For example, U-238, one of the heaviest naturally occurring isotopes has a mass excess of 47.3070 Mev and decays to Th-234 by alpha emission. Th-234 has a mass excess of 40.612 MeV, therefore (Turner 2012):

$$Q_\alpha = 47.3070 - (40.612 + 2.4249) = 4.270 \text{ MeV}$$

Using the Q-value, we can find the energy of the alpha particle:

$$T_\alpha = \frac{234}{238} Q_\alpha = 4.198 \text{ MeV}$$

At times, it is possible to find alpha particles whose energy is larger than what is calculated from the Q-value. This usually occurs with the parent nucleus is a product of decay from a further parent. The parent that is produced from decay can have many different excited states in which most cases, the parent will emit photons to lower itself to a ground state prior to the alpha decay. In some cases though, if the excited state is relatively long lived, thus the decay constant is large for the excited state and the parent may alpha decay directly from the excited state resulting in a Q-value larger than decay from the ground state by the amount of energy equal to the excitation energy.

1.3.2 Beta Production

Beta particles and electrons are interchangeable by properties and characteristics. The major difference is that beta particles are emitted from the nucleus vice the electron cloud. For beta decay to occur, a nucleus must be proton or neutron abundant. For beta

minus decay, which is the concern of this experiment, a neutron decays into a proton, an electron, and an antineutrino. Electric charge conservation requires that if a neutral neutron decays to a positively charged proton, a negatively charged electron must be produced.

The Q-Value for beta decay is the difference between the mass of the parent nuclide and that of the daughter plus one electron.

$$Q = M_p - (M_D + M_e^-)$$

Unlike alpha decay, which results in the production of two bodies, beta particles are emitted in decay into three bodies. The three bodies emitted can all share the energy and momentum which results in a continuous spectrum. The shape of a typical spectrum is shown below.

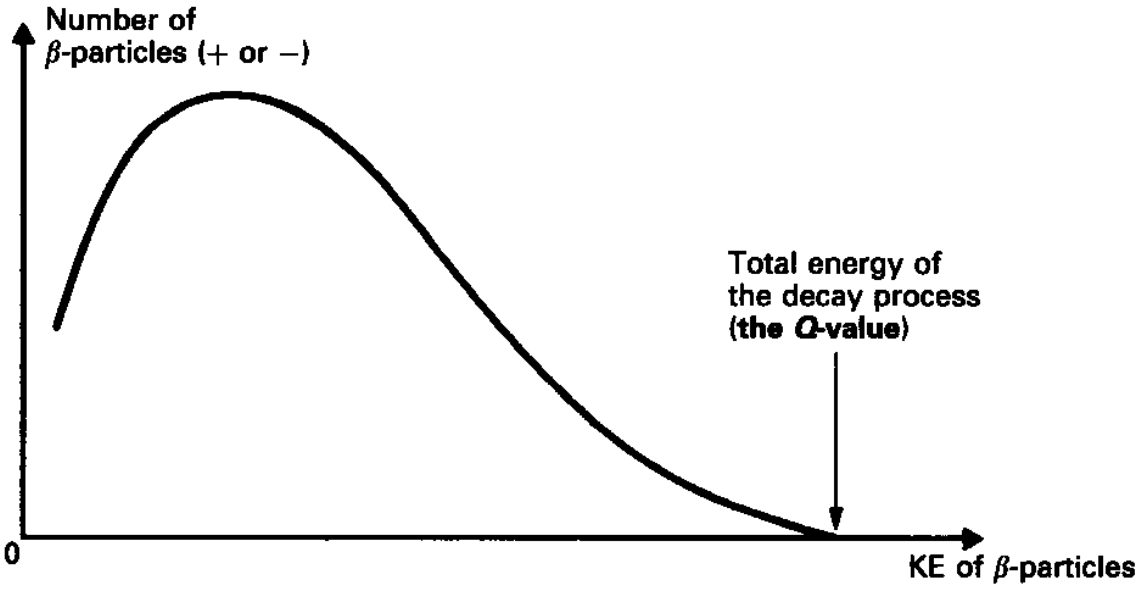

Figure 1 Shape of a typical beta-particle energy spectrum (Turner 2012)

Depending on the relative directions of the momenta of the electron and antineutrino, the energies of the beta and antineutrino can each have any value between 0 and Q. The maximum beta energy is always equal to the Q value for the nuclear transition but as a rule of thumb, the average beta energy is about one-third of Q (Attix 1986). For example we can look at the decay scheme for Co-60. Over 99% of the decays occur with a Q-value of .318 MeV and result in two emitted photons. Every decay must go through an excited state of its daughter Ni-60 with an energy of at least 1.173 MeV + 1.332 = 2.505 MeV above the ground state. When adding the maximum beta energy, you get a total of 2.823 MeV, the total value calculated for a transition all the way to the ground state of the Ni-60 nucleus. Therefore, we can see that the nucleus first emits the beta particle with Q=.318 MeV, followed by the two gamma rays, but which comes first, the 1.332 MeV or the 1.173 MeV? If you look at the decay scheme for Co-60, you can see there is a small .12% chance for a beta particle with a Q value of 1.491 MeV. If you subtract the 1.491 from the total 2.823 MeV, you are left with 1.332 MeV. Therefore, the 1.332 MeV photon must be the last emission before reaching the ground state of Ni-60.

1.4 Alpha and Beta Interactions

1.4.1 Alpha Interactions

Alpha particles are energetic nuclei of helium consisting of two protons and two neutrons bound together. Their mass is relatively large and carry a double positve charge which lowers their penetration ability. Alpha particles will only travel a few centimeteres in dry air before depositing all of their energies along very short path lengths. Because

the electromagnetic interactions extend over rather large distances, it is not necessary for the alpha to make direct contact with an atom to have an effect.

These heavy particles can interact with nuclei by just passing close by. The primary mode of interaction is through coulomb forces between the positive charge of the alpha particle and the negative charge of nearby orbiting electrons. The main methods of interaction are exciation and ionization. Excitation being where the charged particle transfer enough energy to the orbiting electron, thus raising the electron to a higher energy state. When the charged particle has enough energy to overcome the binding energy of the electron ionization occurs by removing the electron and creating an ion pair.

Creation of each ion air, along with direct collisions, requires energy to be lost from the traveling charged particle, therefore, slowing it down. When a heavy particle collides with a lighter particle, only a small fraction of the heavy particle's energy should transfer according to the laws of energy and momentum. The actual amount of energy transferred is dependent on two things: how close the charged particles pass through the atom and the restrictions from quantisation of energy levels.

The distance a charged particle travels before coming to rest is know as range. The range of the particle is not only determined by the intial energy of the particle but also the material the particle is traveling through. Stopping power is a variable used to describe the ionization properties of different mediums. Stopping power is essentially the ratio of the differential energy loss for the particle within the material to it's corresponding path length.

$$S(T) = -\frac{dT}{dx} = n_{ion}\bar{I}$$

T is the kinetic energy of the particle, while n_{ion} is the number of electron pairs formed per unit path length. $\bar{I}$ denotes the average energy required to ionize an atom in the medium. As the particle velocity decreases, the stopping power of the material goes up.

The relativistic version of the stopping power equation was founded by Hans Bethe in 1932.

$$S(T) = \frac{4\pi Q^2 e^2 n Z}{m\beta^2 c^2} \left[\ln\left(\frac{2mc^2\gamma^2\beta^2}{\bar{I}}\right) - \beta^2\right]$$

In the expression above, m is the rest mass of the electron while β expresses the particles velocity relative to the speed of light $\frac{v}{c}$. The gamma is the Lorentz factor, Q is the charge, while Z is the atomic number of the medium and n is the atoms density in volume. Most heavy charged particles, like alphas, do behave nonrelativisticly, therefore, dT/dx is dependent on $1/v^2$ which is explained by the larger amount of time the charged particle spends in the negative field of the electron during low velocities.

Another important characteristic of charged particles can be explained using the Bragg curve displayed in Figure 2 (Turner 2012). We know from the equations above that the stopping power increases as the velocity is lowered which is caused by interactions along the path of the particle. Near the end of the path length of a particle there is a peak in stopping power, at this point, the cross section of interaction increases signficantly before the particle comes to rest. This phenomenon is heavily exploited in cancer therapy using betas as it allows the concentration of stopping energy at a specific point or tumor while minimizing the effects on surrounding tissue.

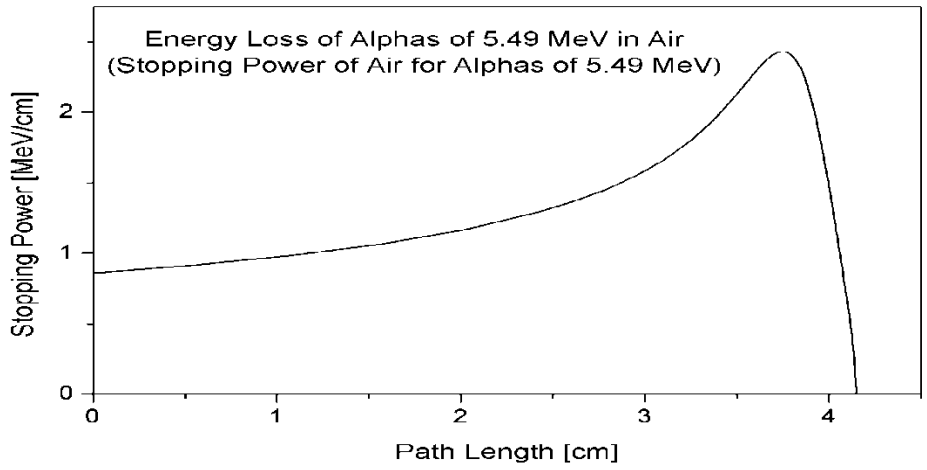

Figure 2 Bragg Peak (Turner 2012)

1.4.2 Beta Interactions

Beta particles are essentially high energy, high speed electrons emitted by beta decay. They interact similarly to the alpha particle as they follow the same charged particle physics but because of the lighter mass and lower charge, they can interact in different ways and have much longer path lengths.

For the purpose of this experiment, we are only concerned with decays involving the emission of an electron. For example:

$$^{234}_{90}Th \rightarrow {}^{234}_{91}Pa + \beta^-$$

The beta particle emitted may go through many types of interactions, inelastic scattering with electrons via excitation or ionization, elastic scattering off of other nuclei, Bremsstrahlung, or Cherenkov radiation. Although a charge particle, due to the mentioned difference in mass and charge of that of alphas, betas mostly reach relativistic energies, therefore the nonrelativistic Bethe formula cannot be used. A derived version of

the Bethe formula is used to explain the energy loss due to ionization and excitation (Attix 1986).

$$-\frac{dE}{dx}=\frac{4\pi k^2e^4}{m_ec^2}\frac{z^2}{\beta^2}\frac{\rho Z N_A}{A}B(v);\quad B(v)=\frac{1}{2}\ln\frac{\tau^2(\tau+2)}{2(I/m_ec^2)^2}+\frac{F(\tau)}{2}-\frac{\delta(\beta)}{2}-\frac{C(I,\beta)}{Z}$$

Other than the collision type interactions mentioned above, betas can also elastically scatter of surrounding nuclei which can significantly change the path of the particle. Compared to an alpha, the beta particle follows a more “zig-zag” path through a medium, therefore, creating a much longer range. This path can be altered by the acceleration or deceleration of the beta particle as it passes near strong magnetic fields. This is known as Bremsstrahlung, or braking radiation. Essentially as betas pass near strong magnetic fields, they can be redirected, changing their path thus creating an acceleration of the particle or deceleration as it changes direction. In classical theory, anytime a charged particle is accelerated or decelerated, it must emit energy. This effect is mitigated when particle energies are below 1 MeV as the energy loss is minimal. The energy loss only becomes significant when the particle energy is above the minimum ionization energy of the medium.

Therefore, bremsstrahlung must be taken into account for determining stopping power as discussed for alpha particles. The equation must take into account these interactions along with the ionizations.

$$\frac{S_l[\text{rad}]}{S_{\text{m}}[\text{ion}]}=\frac{1}{E'}ZE$$

To summarize, below is a graph illustrating the fractional energy loss per radiation length in lead as a function of electron energy.

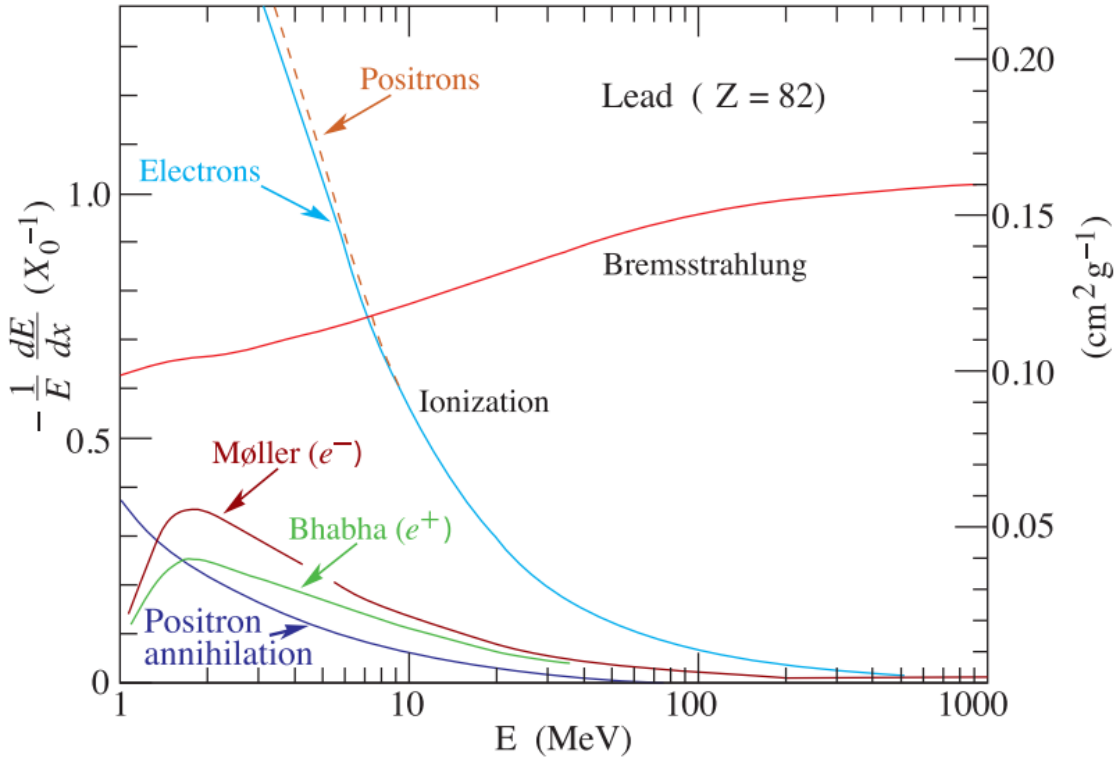

Figure 3 Fractional Energy Loss per Radiation Length in Lead (http://pdg.lbl.gov/)

The last major interaction of beta particles is Cherenkov radiation. This type of radiation is electromagnetic radiation emitted when a charged particle moves through a dielectric medium at a higher speed than the phased velocity of the light found that medium. Even at high energies, the loss of energy from Cherenkov insignificant when compared to other interactions such as collisions and bremsstrahlung.

1.5 Alpha and Beta Detection

A very simple system can be built to detect charged particles, including electrons released as a alpha interacts with the medium or wall of the device. The major components include an anode, a cathode, a power supply, and output circuitry such that a registered pulse is displayed as a count on a meter.

Scintillation detectors use light produced from inozing events in order to report results. The light is emitted as the radiation interacts with a certain type of liquid or crystal. Flourescence occurs when light is emitted by the scintillation material after is enters an excited state following ioniziation. This light is is measured by a photocathod and photomulitplier tube in which it is then converted to an electrical signal. For semiconductors, a photodiode is used instead. The electrical signal is then transferred to the instruments readout.

Scintillators consist of both organic and inorganic materials. Inorganic scintillators have crystals ususally grown in high temperature furnaces and are made of alkali halides. The structrure alone is what creates the energy bands between in which electrons can move between energy levels due to excitation or de-excitation. Organic scintillators are composed of aromatic hydrocarbons. Unlike inorganic scintillators they scintillate on a molecular level and no structure is needed. Liquid scintillators are essentially fluid solutions composed of the organic compounds. Liquid scintillators provide a 4π geometry since the isotopes being counted are dissolved in the solution with the scintillator. A plastic scintillator is comprised of a solid solution of organic scintillating molecules in a polymerized solvent. This research project has used a Passivated Implanted Planar Silicon Detector for both alpha and beta detection.

For solid state detectors, Germanium and silicon are the most widely used materials Is solid state detectors, the electrons in the valence band are bonded to the crystal lattice while the electrons in the conduction band are able to freely move through the structure. The energy required electrons to move between the valence and conduction band gives it it's classification. The classifications typically used are , conductor (gap energy << 1 eV such as copper), insulator (gap energy > 5 eV such as rubber), or semiconductor (gap energy about 1 eV) (Lee, Kang, Jang and Kim 2011).

In semiconductor scintillators, energy deposited by the ionizing radiation excites the electrons which forces them to move from the valence band to the conduction band. The movement of electrons forms an electron-hole pair. Once the electrons move to the conduction band, they will flow towards the positive terminal of the detector which results in a pulse via a corresponding electronic system. The holes left behind are then filled by additional electrons still trapped in the valence band.For n-type semiconductors, the number of electrons in the conduction band are increased by doping the crystal with impurities causing a large imbalance between the number in the valance band. This is done to ensure more charge carriers are available than holes. In a *p-type* semiconductor, an impurity is added which creates a deficiancy of electrons in the valence band. In n-type the majority carriers are the charged electrons increased in the conduction band where as in p-type, the reduced amount of electrons in the valance band causes the holes to be the majority carrier.

Liquid scintillation detects charged particles using the same light emitted in solid scintillation. The main difference is that the scintillation effect takes place within a solution rather than a solid crystal. This allows close contact between the isotope being

counted and the scintillation material. The scintillation cocktail absorbes the energy emitted by the radioisotopes and re-emits it as flashes of light. This effect can only be accomplished via the benefit of a two part solution, the solvent and the phosphor. The solvent absorbs most of the energy from interactions while the molecules of the phosphor, that are dissolved in the solvent, convert the absorbed energy to light. Most newer cocktails use other materials and solutions to extend the range of the interactions of different sample compositions.

The solvent comprises of 60 to 99% of the total solution (Wilkinson 1950). When a radioisotope is dissolved in the sovlent and undergoes an emission event, the particle or ray will usually interact with solvent molecules before its energy is gone. Therefore, the solvent must be efficient at storing the energy and transferring it to the phosphor molecules instead of dissapating the energy by other means. The energy abosrbed by the solvent will passed along to nearby solvent molecules until it can be transferred to a phosphor molecule which re-emits the energy as light.

The phosphor molecules usually consist of .3 to 1% of the solution and are the primary means of converting the captured energy to emissions of light. The scintillation molecules seems to produce a dipole moment in their solvation shell. This allows direct transfer of energy betweent the excited solvent molecules and the scintillator by up to a factor of 10. Most scintillators emit light below 408 nm, which for early photomultipier tubes, the response dropped signficantly. Modern phototubes are now more capable of counting light pulses in this range, at times a secondary scintillator is added to improve efficiency.

1.6 Examples of Alpha and Beta Detection

1.6.1 Solid State Scintillation

Silver activated zinc sulfide, ZnS(Ag), is one of the oldest inorganic scintillators and has a very high efficiency, comparable to NaI. ZnS(Ag) is widely used to measure alpha radioactivity in environmental samples but can also be used for other heavy ion detection. Because of the varying energies involved with DU, and the need to determine the activity contributed also by the betas, a silicon detector would have better results.

The silicon charged particle detector is a wafer of silicon having contacts forming the p-n junction. For Surface Barrier Detectors, these contacts for surface barriers or can form a junction in the more modern Passivated Implanted Planar Silicon (PIPS) detector. A bias voltage is first applied in the reversed direction. This establishes an electric field across the device. The reverse bias creates a depletion region with no free charges; therefore, to function as a particle detector, the region needs to be thicker than the penetration range of the particles being detected (about 32 microns for 6 MeV alpha particles in silicon)((Lee, Kang, Jang and Kim 2011). With the alpha energy ranging from 4 to 5 MeV, the LUDLUM 3030P's thickness of this region was adequate for determining a count rate.

During the detection process, the particle stops in the depletion region, forming electron-hole pairs. The energy required to form a single electron-hole pair is independent of the energy of the particle but is determined by the material used. The number of electron-hole pairs formed is directly proportional to the energy of the stopped particle. The electric field applied in the region allows the movement of electrons to one terminal and the holes to another, this creates a charged pulse that is integrated in a

preamplifier which creates the observed voltage pulse. These pulses are then fed to a multichannel analyzer which serves as a pulse height analyzer and converts the analog pulses to digital values. In order to properly display alpha and beta counts simultaneously, multiple channels must be used and the pulses sent to each corresponding channel based on their heights.

These two detection methods will allow us to quantify the amount of contributed beta and alpha activity per unit mass from all isotopes found in Uranyl Nitrate. LSC will be able to tell us the total counts per unit mass within the prescribed energy window of .1 to .5 Mev based on a standard curve. The mass can then be used to determine the relative activity for each alpha and beta based on a standard curve created by counting different masses on the alpha/beta counter.

1.6.2 Liquid Scintillation

The principal use of liquid scintillation counting is the determination of low-every beta emitting nuclides, but it has been known since the early 1990s that alpha particles could be counted effectively using the same technique. Alphas create less excitation energy transfer due to their relatively large mass and higher charge.

The light emitted from alpha particles in the liquid scintillation cocktail is about one tenth of the light intensity per unit of the particle energy for the beta particles (Kessler 2012). All of the uranium isotopes of DU are alpha emitters while the short lived daughters of U-238, Th-234 and Pa-234m, are beta emitters. The alpha particles from U-238 and U-235 decay have energies of 4.20 and 4.40 MeV respectively. These energies are much higher than the maximum energies for the beta of the decay daughters, but the

photons produced in a liquid scintillation fluid produced by the dissipation of alpha particle kinetic energy will be comparable to that of the beta particles of energies at around 0.35 MeV (Bower, Angel, Robinson, and Smith 1994) .

Broad energy bands will overlap the narrower, monoenergetic uranium bands in a liquid scintillation spectrum; therefore, determining the amount of uranium in a liquid scintillation solution can lead to erratic results if the beta activity is not accounted for. Fortunately, for the purpose of this thesis, we will take into account all particles deposited by DU and determine the total uptake based on the total counts accumulated within the energy window of .1 MeV and .5 MeV. This window will capture all decay reactions within the DU progeny.

Liquid scintillation involves the process of a radioactive sample in uniform distribution within a liquid medium being capable of converting the kinetic energy of the emissions into a form of light. Particles emitted by radioactive decay deposit energy as it undergoes interactions within the fluid. This loss of kinetic energy is absorbed by the solvent molecules which puts them into an excited state. The excited solvent molecules will then return to its ground state by emitting UV light in the process. The excited solvent molecules can also transfer energy to each other and the solute (fluor); this disturbs the orbital electron cloud of the solute and raises it to a state of excitation. As the electrons return to the ground state, a photon in the form of UV light is emitted and is absorbed by the fluor molecules which then emit blue light flashes as it returns to its ground state. These nuclear decay processes produce approximately 10 photons per KeV of energy and the intensity of the light is proportional to the particles initial energy (National Diagnostics Laboratory 2012).

There are many factors that affect the results of the light emitted versus those that are counted by the photomultiplier tube. Quenching is the reduction in system efficiency as a result of energy loss in the scintillation fluid. The three major types of quenching are photon quenching, chemical quenching and optical or color quenching. Photon quenching occurs when there is an incomplete transfer of particle energy to the solvent molecules. Chemical quenching is apparent when the energy is absorbed before it is converted to photons while color or optical quenching results from the passage of photons through the liquid. Color quenching depends on the color of the fluid and the photon's path length. These effects will be apparent in our samples as the available LSC does not have the ability to discriminate alpha and beta radiation, provides no reliable quench curve for uranyl Nitrate, and will be more susceptible to color quenching as dissolved tissue will change the density and color of the sample.

Due to the limitations of available liquid scintillation counters, another method of determining the absorbed activity had to be used. Some liquid scintillation counters have refined Alpha/Beta discrimination using a pulse-decay analysis. This sensitive technique for discriminating between the two particles is done by measuring the anode pulse decay characteristics of the alpha and beta events by sorting the pulses into separate multichannel analyzers. When this method is combined with time-resolved background discrimination, the misclassification of alpha as beta and beta as alpha is reduced. Due to the inability to develop a unique quench curve without standard activity samples, no curve was developed and counts only were used to relate the mass of DU absorbed.

1.7 Counting Statistics

There is some statistical variability that occurs with the decay of radioactive atoms and the detection of these interactions. Radioactive decay follows a normal distribution, a bell shaped curve symmetrical about the mean,$\bar{x}$ shown in Figure 4.

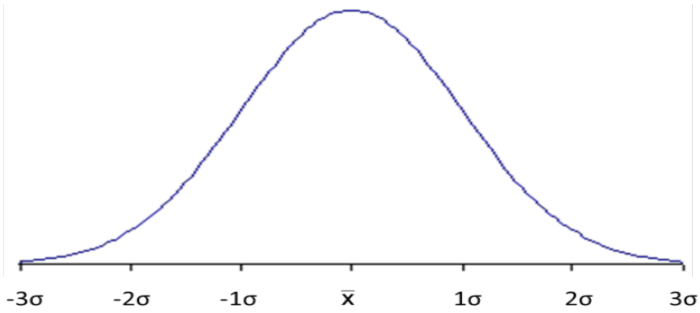

Figure 4 Radioactive Decay Distribution

The area under the curve represents a sample of the population involved in the study. The x-axis represents the number of standard deviations from the man which correlates to observed values. The y-axis is the frequency of the observed values with most values falling under the curve close to the mean. (x). The area between -1σ and 1σ is 68% of total and between -2σ and 2σ is 96% of total.

For measured counts, *n*, is a period of time, *t*, the count rate, *r*, is given in counts per minute (cpm). The standard deviation of the count rate is

$$\sigma_r = \frac{\sqrt{n}}{t} = \sqrt{\frac{r}{t}}$$

and a count of radiation for some time is presented as $r \pm \sigma_r$.

The total counts of a sample over a given period of time include; the count rate of the sample, and those registered from natural background radiation. Therefore, for accurate readings, background is also counted for a period of time with the detector in the

same location. This alleviates any skew in the background readings and removes any effects the sample has on the count rate. The net count rate, r_n, is calculated by subtracting the background count rate from that of the sample. The standard deviation of the net count rate is then:

$$\sigma_n = \sqrt{\frac{r_g}{t_g} + \frac{r_b}{t_b}} = \sqrt{\sigma_g^2 + \sigma_b^2}$$

where r_g is gross sample count rate, t_g is gross sample count time, r_b is background count rate, t_b is background count time, σ_g is standard deviation of gross count rate, and σ_b is the standard deviation of background count rate.

The efficiency of a detector or counting system, ε, is determined by counting a known a radioactive source with a known activity and calculated by:

$$\varepsilon = \frac{cpm}{dpm}$$

where *cpm* is the detected net counts per minute and *dpm* is the calculated disintegrations per minute of the radioactive source (*1 dpm = 60 Bq*). Solid State scintillation detectors have efficiencies of only of varying values depending on the particle being detected, while a liquid scintillation system can approach 100%. This does not consider the geometry of the sample as any source emits radiation isotropically and thus resulting in roughly half of the interactions being registered on a solid state detector. The benefit of using the LSC in this study is that it allows for full 4π counting.

1.8 Overarching Goals and Significance of this Study

Due to the growing use of charged particles in therapy and increasing awareness of the existence of background radiation, it is important to study the long term effects of these particles. The zebrafish model has been used extensively recently for many studies ranging from behavioral effects of toxicants to helping define the genetic and epigenetic mechanisms of toxicity to a broad range of elements.

By distinguishing the distribution of heavy metals and using radiation detection methods to track their accumulation, future studies can be used to evaluate the combined effects of such metals and common everyday exposures. Lead, for example, is commonly found throughout everyone's day to day activities. Although recent regulations and limitations have reduced the overall population exposure, being able to distinguish the effects from lead alone and those combined with other environmental or therapy related charged particle interactions will only increase the knowledge of the science field and provide more information to the general public where these exposures may be of concern.

This study is purposed to calculate the bioconcentration of DU in zebrafish using radiation detection and compare it to that of known human distribution, while also comparing dose conversion factors for known isotopes found in DU to the theoretical dose calculated for the fish. These important factors will then allow long term studies with much lower concentrations combined with other common non-radioactive elements and the behavioral and neurological effects they may have.

To accomplish these goals, determination of the sensitivity of the liquid scintillation counting system was performed. Separate groups of larvae were exposed to multiple concentrations of uranyl nitrate. During exposure their death rate and behavior

was noted and at the end of seven days, all larvae were dissolved and counted at different numbers to determine sensitivity. After a correlation was made between the counts seen on the LSC with the corresponding mass of uranium, a plastic scintillator was used to observe the relationship between the counts on the LSC and those recorded from the plastic scintillator. Standard curves were then developed between the two instruments. Finally, once the correlation was made, adult zebrafish, after exposure, were dissected and counted using the LSC to determine the distribution of uranium throughout the body.

CHAPTER 2. MATERIALS AND METHODS

2.1 Use of Uranyl Nitrate

Uranyl Nitrate, in the form of $N_2O_8U•6H_2O$, exists in a crystalline form. It is made from DU which may lead to heavy metal toxicity along with radiation toxicity. DU is usually not considered a dangerous radiological substance but in large quantities, it has the potential for harm. There have been no reputable reports of cancer or other negative health effects from radiation exposure to ingested or inhaled natural or depleted uranium (Bleise, Danesi, and Burkart 2002). DU does have a chemical toxicity similar to that of lead, thus inhaling fumes or ingesting some form of oxides is considered a health hazard. In the human body, most uranium is excreted within a few days while the remaining is absorbed into the bones and kidneys. Because of these hazards the World Health Organization has set a daily intake level of .6 microgram/kg of body weight.

DU is the waste product from the enrichment process of U-235 and its subsequent removal from natural uranium or fission processes. These processes lower the radioactivity of DU compared to that of U-238. Natural uranium exists with concentrations of U-235 of about .7% and U-234 at around 0.0053% (IAEA 1989). Once depleted, the contribution from U-235 and U-234 are lowered to around 0.2% and 0.0008%

respectively. Also, the activity contributions from the different forms of uranium change significantly.

For natural uranium, U-238 contributes only 48.9% of the activity, while U-234 is roughly the other 48%, with U-235 providing the remainder. The activity from U-234 is much lower in DU as it gets depleted to a lower ratio due to its atomic weight. The outcome of these processes alters the activity distributions of the uranium itself. For natural uranium, after about 1000 years, U-238 and its daughters exist in equilibrium until the parent completely decays away; DU on the other hand, has its contributions reset by the removal of U-235 and U-234. The majority of the daughters do not add to the total activity until U-234 has adequately built up again from the decay of Th-234 and Pa-234m. For this study, we are assuming that U-238 and its direct daughters, Th-234 and Pa-234m, are the major contributors to dose while U-234 only contributes approximately 14% and U-235, about 1% (wise-uranium.org 2016).

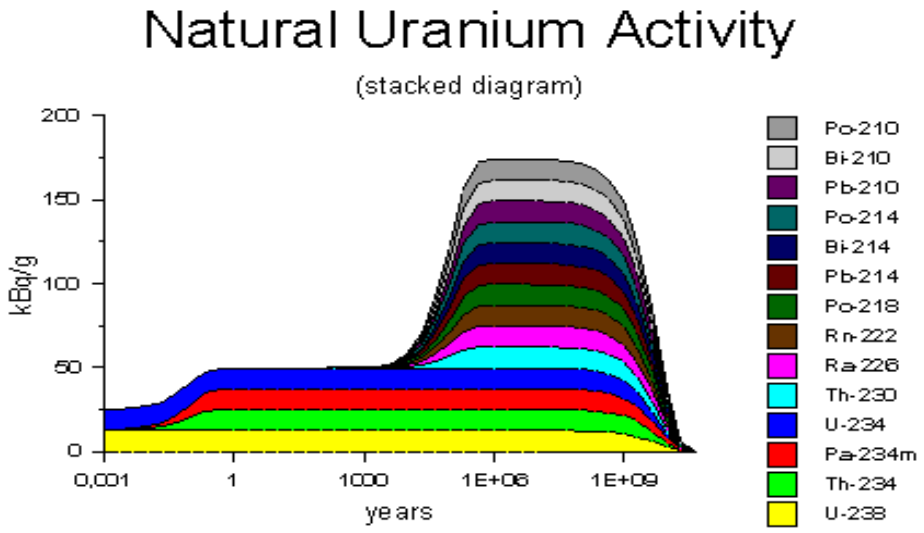

Figure 5 Natural Uranium Activity Contributions (wise-uranium.org 2016)

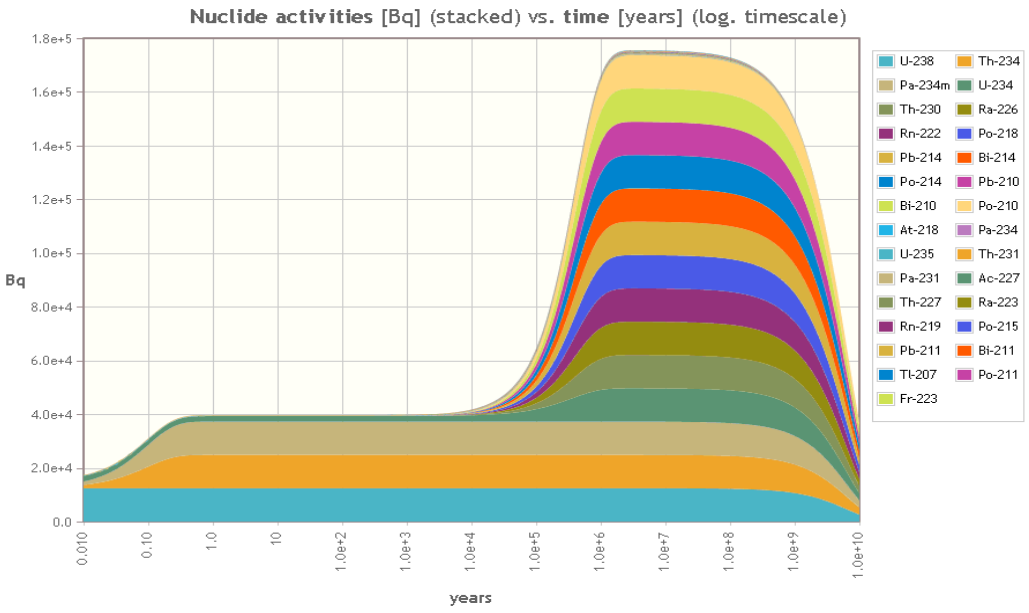

Figure 6 Depleted Uranium Activity Concentrations (wise-uranium.org 2016)

Uranyl Nitrate is normally used for heavy metal electron microscopy staining. In tissue, it stabilizes nucleic acids and membranes when used prior to embedding procedures and is frequently used to “post stain” which further enhances the contrast of the membranes. Uranyl salts are also used as negative stains for viruses and small cellular organelles in suspension. Its relative solubility in water made it a reasonable source to track the distribution of activity throughout the experiments.

2.2 Zebrafish Model for Alpha and Beta Exposure

2.2.1 Care and Handling of the Zebrafish

One of the most important aspects of any animal studies is to reduce animal suffering. This is accomplished in two main ways: use the least sentient organism

possible to answer the question and the ease of being able to provide an environment as close to the organism's natural habitat as possible to reduce stress.

The zebrafish has become one of the preferred vertebrate model systems in biomedical research. Several features make the zebrafish a unique vertebrate model for toxicological studies including: the short generation time, high fertility, external fertilization, *ex utero* embryonic development, transparent embryos, small size of adult organism, a short life span, and relatively low-costs associated with maintenance. In this study we are observing the metabolic process of internal exposure to DU found in uranyl nitrate. This will allow future studies of genetic and epigenetic mechanisms of a developmental lead exposure combined with alpha exposure that is representative of environmental exposures to the human population. Firstly, we are identifying the distribution of the DU which will allow us to relate specific exposure concentrations to organ and whole body doses received. Once a dose model is developed, it can be compared to that of humans which will then allow further studies on the effects of low dose alpha exposure when combined with other common exposures being studied.

In this study, we used wild type AB strain zebrafish from the Freeman Lab. This colony was initially established from AB zebrafish purchased from the Zebrafish International Research Center stock center (www.zebrafish.org). Adult AB zebrafish were bred following standard protocols to produce embryos (Westerfield M. 2007). Uranyl Nitrate solutions was prepared following routine procedures in water. The stock solution was within solubility limits and thus, no solvent was needed. To attain final exposure concentrations, the stock solution was diluted to final concentrations of 0.001 to 1 uCi/l. These concentrations correspond to similar levels present in environmental

settings such as mining, industrial plants, and the environment and result in a low dose exposure in the fish. The concentrations of the Uranyl Nitrate were determined by producing a calibration curve of the solution versus counts read by a liquid scintillation detector and an Alpha/Beta PIPS counter prior to being introduced to any colony of fish. Fertilized embryos ~1 hour post fertilization (hpf) from multiple mating sets were collected, pooled, and assigned to a treatment group to consist of one replicate. As zebrafish embryonic development is *ex utero*, this provides great ease in accurate exposure concentrations in comparison to mammalian models.

This study used a unique exposure regimen to assess the distribution of the alpha particles and its lifespan impacts from developmental radiation exposure and do not unnecessarily duplicate previous experiments. A genetic model that is similar to humans, yet in which lifespan impacts of a developmental chemical exposure is needed for future studies. The zebrafish presents an alternative and complementary model to rodents to conduct this experiment and presents ease in dosing as embryonic development is *ex utero* and adult fish are easily contained and controlled.

The objectives are to determine the distribution of DU within the organ systems of the zebrafish and see if there is a correlation between the amount of DU absorbed and the mass of the fish. In order to further study the effects of combined exposures, i.e. exposures to lead and alpha or any other toxic substances, a representative dose model will need to be calculated strictly for the ingestion/inhalation of alpha particles alone. This study determines the metabolic distribution of contaminants which will help define the genetic and epigenetic mechanisms of toxicity of this exposure along with other toxic chemicals during development and the later in life impacts of this

developmental chemical exposure on the central nervous system. This study requires a vertebrate model system so that the immediate developmental changes and lasting impacts throughout the life span can be investigated. The *ex utero* embryonic development and relatively short life span of the zebrafish provide distinct advantages in this study. Moreover, a plethora of genetic tools are developed for the zebrafish that can be utilized in future study including a complete zebrafish genome sequence. It is estimated that zebrafish genes are ~80% homologous to human genes and permits translation from the zebrafish model to humans (D'Costa, A. and I. T. Shepherd 2009 and Howe M., 2014).

Water used in our fish system is from a reverse osmosis (RO) water supply. These fish were maintained in 2 liter bins with no more than 10 fish per tank. For the period of 7days for exposure, oxygen was supplied to each flask via an air pump to ensure adequate mixing of our solution and proper oxygen levels for the fish. Temperature was maintained in each tank by having all bins surrounded by water with a circulation pump and heater to maintain temperature between 25°C - 28°C.

In the main system, the fish are maintained in flow through systems with an approximate 10% water change each day. Each system is self-contained for filtration (particulate, carbon, and biofilter) and disinfection (with an ultraviolet light source). pH levels are stabilized with the use of aragonite. The following water quality parameters are monitored in our systems:

- Temperature: 25°C - 28°C (ideal is 28°C) –daily
- Conductivity: 300-600 µS (ideal is 500 µS) – 2-3X per week
- pH 7.0 to 8.0 (ideal is 7.5) – 2-3X per week

- Nitrite and Nitrate: 0 ppm (Nitrite <0.75 ppm; Nitrate <20 ppm) – 1X per week
- Ammonia: 0 ppm (<0.8 ppm) – 1X per week
- Chlorine: 0 ppm – 1X per week
- Dissolved oxygen: 7.8 ppm (7.3 to 8.3 ppm) – 1X per week
- Salinity: 0.25 to 0.75 ppt – 2-3X per week
- Hardness: 75-200 mg/L $CaCO_3$ (zebrafish are a hard water species that prefer 100 mg/L $CaCO_3$) – 1X per week

Because of the chemical requirements to ensure an adequate environment, each batch was only dosed for a maximum of 7 days. Because of the activity concentrations, the individual tanks could not be connected to the main system used for the colony, therefore, ensuring the chemical specifications were correct prior to adding the fish to the tanks and limiting the time endured in the semi stagnant water was important. pH was determined in each tank after the concentrations of uranyl nitrate was added to ensure it remained in the specified range. Fresh RO water was added daily in 5 to 10 mL increments during feeding times to ensure water levels remained relatively constant due to evaporation.

Once each dose regiment was complete, the fish were removed from each tank and separated into groups and placed in fresh water from the main system. Since all specimens were older than 8 days post fertilization (dpf), euthanasia was performed by submersion in ice water for at least 10 minutes in accordance with the American Veterinary Medical Association (AVMA 2013) guidelines. When opercula movement was verified stopped, each batch was returned to fresh water to observe opercula

movement and ensure no revival. Then they were rinsed off with RO and prepared for organ removal or for vial counting.

2.2.2 Dose Regimen of Zebrafish

Depleted uranyl nitrate, $N_2O_8U•6H_2O$, was purchased from SPI supplies. All other reagents of analytical grade were supplied by Fisher Scientific, with the exception of 30% hydrogen peroxide solution, which was obtained from National Diagnostics.

Initially, groups of 50 larvae (10 dpf) were exposed to three concentrations of uranyl nitrate, 0.1 uCi/L, 0.5 uCi/L, and 1.0 uCi/L or a control treatment for a period of 7 days with one tank per treatment group. Each tank contained 500 mL of water with 25 mg of tropical larvae supplement and 3 mL of concentrated paramecium cultured from wheat kernels and brewer's yeast added daily. Based on the manufacturer's information, the specific activity of our uranyl nitrate was approximately0 .3 uCi/L, this value was an average over the entire batch. Therefore, to achieve the desired concentrations, 333.3 mg, 1.7 g, and 3.3 grams were added to each tank respectively.

Survival rate was observed and compared to the average survival rate of 5 to 10% per batch. Those dosed to 1.0 uCi/L yielded 100% lethality after just a couple of hours. 10% survival was noted for those dosed to 0.5 uCi/L, while the group exposed to 0.1 uCi/L seemed to be within the normal survival rate of 5 to 10% for that particular age group. It was assumed that the larvae would be more susceptible to the toxicity of the DU itself so any adult zebrafish exposed to similar concentrations should have a better survival rate. Those that survived were collected, euthanized, pooled (one pool per treatment) together and counted using a Liquid Scintillation Detector (LSC). This step

was used to determine the viability of the LSC in tracking the distribution of uranyl nitrate while also providing a high enough concentration for detection to achieve the best survival rate for the adult zebrafish. Three additional groups were exposed at 50 larvae per batch using the same environmental conditions. The concentrations of exposure were 0.005, 0.01, and 0.02 uCi/L along with a control group and counts recorded from the LSC.

The next experiment used adult fish aged to 3 months post fertilization (mpf). Due to the limited survival above 0.1 uCi/L and the extensive time it takes to raise them to the correct age, 4 treatment groups of 10 were prepared, 1 control group, .03 uCi/L, .05 uCi/L, and .1 uCi/L. There was one tank per treatment with 10 fish in each tank. All groups were observed to have 100% lethality within a couple of hours. The assumption that the larvae would be more susceptible was seemingly false as the adults exposed to lower concentrations had a higher lethality rate. In order to ensure this was correct, another 4 batches of 3 fish each were exposed to even lower concentrations to confirm.

Based on lethality, at these exposure concentrations an additional experiment was started that included exposures at 0, 0.01 uCi/L, 0.015 uCi/L, 0.02 uCi/L, or 0.03 uCi/L. The group exposed to 0.01 uCi/l had 100% survival over the 7 day period, the group exposed to 0.015 uCi/L were all deceased within 8 to 16 hours post exposure, 0.02 uCi/L were all deceased between 3 and 4 hours, and the 0.03 uCi/L showed 100% lethality within 3 hours confirming our results from the first set of exposures.

To ensure survival and adequate activity to be absorbed and counted by LSC, final exposure concentrations were set at 0.001 uCi/L, 0.005 uCi/L, and 0.01 uCi/L, equating to 3.3 mg, 16.7 mg, and 33.3 mg respectively added to 1 L of water. There was one tank per treatment with each tank containing 8 fish. After 7 days of exposure, the fish

were removed and euthanized in accordance with AVMA guidelines, five fish from each treatment were dissected to retrieve the brain, skeletal systems, cardiovascular system (liver, heart), and intestines. Due to the low activity of DU, groups of 5 organs were pooled together in order for adequate counts to be measured by the LSC. Only organs of the highest exposed groups were collected. The remaining fish were individually removed, weighed and counted.

It was decided to use Biosol provided by Fisher Scientific to alleviate the color quenching. Each sample was homogenized with an ultrasonic homogenizer in each sample vial and 1 mL of Biosol was added to each vial. The tissue mass may represent some quenching in the LSC. At first, tissue samples from the larvae were dissolved in a nitric acid solution using UV light and 30% hydrogen peroxide solution was used to reduce the color but the sample were still too yellow to get consistent results. The vials were then placed in an incubator at 50 °C for at least 4 hours. Depending on the dissolved tissue color constraints, very faint brown to light brown, .1 to .2 mL of 30% hydrogen peroxide solution was added and the samples were allowed to sit for at least an additional hour. Once samples seemed to be clear, 10 mL of Bioscint scintillation solution, provided by Fisher Scientific, was added to the sample. Each sample was counted 3 times using a Perkin Elmer TriCarb 2800 LSC for 30 minutes.

2.3 Liquid Scintillation Counting Techniques

It is understood that LSC can be close to 100% efficient at counting alpha activity. Since DU decays with both alpha and beta emissions, an LSC platform would be appropriate for counting the activity in the samples, even at very low concentrations. A

Perkin Elmer TriCarb 2800 LSC was used for all standards and samples. This is the most basic platform for LSC counting so it was required to couple the results with a PIPS alpha/beta counter.

The biggest obstacle for counting samples containing uranium combined with tissue was quenching. The amount of uranyl nitrate required for significant activity levels gave the samples a yellow color that resulted in nearly 90% quenching effects. The addition of tissue mass though dissolved also added to this effect. Because of time restraints, a thorough quench standard was not performed, mostly due to the activity of our source being an average over many vials of the uranyl nitrate, and having to consider the effects of color and mass. Quenching essentially forces the energy curve to the left of where it should be, this makes it hard for a correct DPM to be calculated as the efficiency is off for every sample of a different shade or for every different amount of tissue dissolved. Also, because of known quenching effects, the lower energy beta particles from the decay of Th-234 may be pushed to below the pulse threshold.

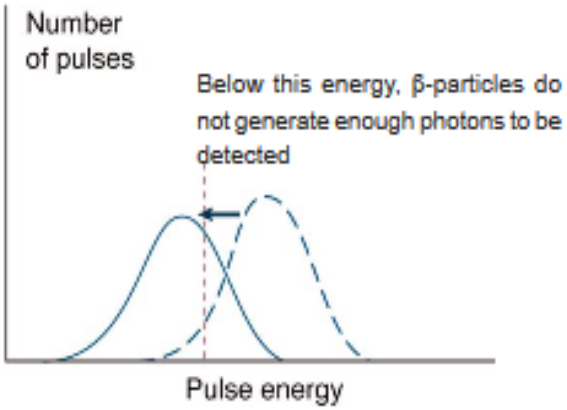

Figure 7 Quenching Effects on Energy Spectrum (National Diagnostics Lab 2012)

It is known that alpha emission from uranium as seen on an LSC are not seen at the corresponding energy ranges. The light emission from these alpha energies (U-238, U-235, U-234) occur in the energy window around 150 to 500 keV, which happens to be the same region the Th-234 beta is released in. Some sort of alpha extraction method could be used but for the purpose of this study, we wanted to take into account all counts recorded.

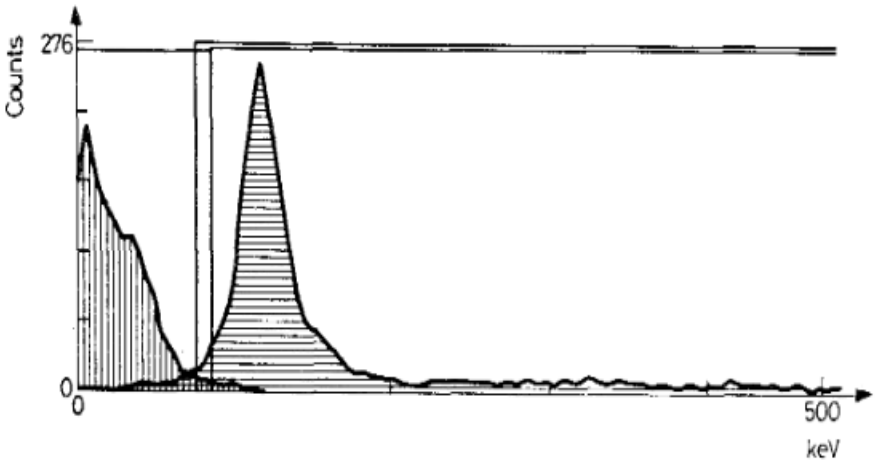

Figure 8 Spectrum of Uranyl Nitrate (Bower, Angel, Gibson, and Smith 1994)

With the lack of a proper quench curve to account for the difference in mass or volume, standard solutions were made using different volumes of water along with different amounts of dissolved tissue to assess the effect of quenching. Eight different concentrations were added at three different volumes: 0.001,0.005, 0.01, 0.015, 0.02, 0.5, 1, and 2.1 uCi/L in 1, 2, and 3 mL volumes. Each sample contained 1 mL of Biosol, .15 mL of 30% hydrogen peroxide solution, and 10 ml of the Bioscint scintillation fluid. Since there was no way to accurately get the correct DPM, these ranges gave us a way to correlate the counts that were read to the mass of DU in each vial. Any discrepencies

would be noticed due to the variance in volumes containing the same mass of uranyl nitrate. All activity concentrations were calculated based on the 0.3 uCi/g specific activity given to us by the vendor.

2.4 Ludlum 3030p PIPS Counter

Since the method used for the LSC would not give us an accurate activity based on the counts seen, another method needed to be used in order to correctly calculate activity absorbed. The 3030p is a solid state PIPS detector that can be used for simultaneous counting of both alpha and beta activity. Because detector efficiency must be calculated for pure alpha and beta emitters separately, a uranium standard could not be used.

DU is mostly composed of U-238, Th-234, Pa-234m with traces of U-234 and U-235 based on age and depletion methods. Our source of uranyl nitrate came with an average of approximately 0.2% U-235 by mass. We used the average weight and activity contributions for DU and due to the age of the source, 1 to 10 years, the activity contribution from Th-234 and Pa-234m should be equal to that of the U-238 due to equilibrium. U-235 contributes approximately 1.1% of the activity while U-234 contributes around 14.2% (wise-uranium.org 2016).

Composition of uranium isotopes in depleted uranium from enrichment of natural uranium

(from enrichment to 3.5%, tails assay of 0.2%)

	U-234	U-235	U-238	Total
weight %	0.0008976%	0.2%	99.799%	100%
activity %	14.2%	1.1%	84.7%	100%
activity in 1 g U_{dep}	2,076 Bq	160 Bq	12,420 Bq	14,656 Bq

Figure 9 Composition of Uranium found in Du (wise-uranium.org)

For an average specific activity of 0.3 uCi/g, we can calculate what the theoretical activity should be for one gram of our uranyl nitrate. 84.7% of the activity is due to U-238, therefore, since our source is in equalibrium, the contribution from Th-234 and Pa-234m should be equal. U-235 will contribute to 1.1% of the activity while U-234 will provide 14.2% of the activity. At 84.7% of the activity, U-238, Pa-234m, and Th-234 should each contribute .2541 uCi/g with U-235 adding 0.0033 uCi/g and U-234 at 0.0426 uCi/g giving a total of 0.8082 uCi/g when counted. Since the 3030p has the ability to display CPM or DPM based on efficiency calculations, the above was converted equal 1794.204 dpm/mg.

Because of the age of the sample, we know there are not any significant contributions from the decay of U-234 and U-235. This lets us focus on the decay of U-238 as a majority of the activity.

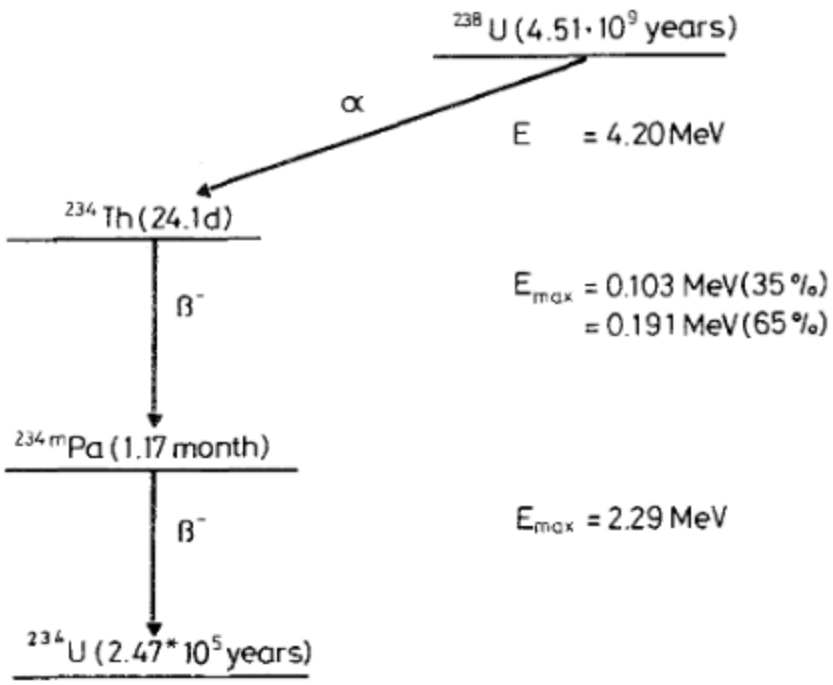

Figure 10 U-238 Decay Chain to U-234 (Bower, Angel, Gibson, and Smith 1994)

Since a U-238 standard could not be used due to multiple particles of both alpha and beta being emitted simultaneously, efficiencies for isotopes with equivalent energy levels was used. The 3030p has an alpha efficiency(4π) of 35% for Pu-239 which emits an alpha with an energy level of around 5.2 MeV which is fairly close the energy levels of U-234, U-235, and U-238 at energy levels between 4 and 5 MeV. For betas, the 3030p has an efficiency of 15% for Tc-99 and 34% for Y-90. The beta energy level for Tc-99 is aroudn 140 keV which is close to the beta energy of Th-234, and the beta energy for Y-90 is just over 2 MeV which is within acceptable range of the beta decay energy of Pa-234m.

2.5 Dose Conversion for Absorbed Activity

Absorbed dose is a measure of the amount of energy being deposited by ionizing radiation in the mass of a material. The ICRU has defined absorbed dose as D= Δε/Δm, where Δε is the mean energy deposited by the radiation to a mass Δm. The SI unit to measure absorbed dose is the gray (Gy) which is equal to J/kg and can be used for any type of radiation.

A radionuclide that is ingested or inhaled is considered an internal emitter. Since we are looking at the alphas and betas deposited by the isotopes of interest, we can assume their energies will be absorbed in the tissue that contains them. For the purpose of this report, the absorbed dose rate will be calculated based off of the activity of each nuclide found in specific organs.

$$\dot{D} = A\overline{E}\,\frac{MeV}{g\,s}\,x\,1.60\,x10^{-13}\,\frac{J}{MeV}\,x10^{3}\,\frac{g}{kg}$$

With the equation above, and the branching ratios of the isotopes in the decay chain, we can us the activity calculated per nuclide and apply the equation to come to a dose distribution of each isotope. For example, if one fish liver was found to have 1000 Bq of U-238 activity and the liver weighed 1 mg. Using the average energy of the alpha emitted during U-238 decay as 4.2 MeV, that would be equivalent to 6.72E-4 Gy/s or 58 Gy per day (ICRP 72).

Due to the weight of individual organs, a total of 5 fish from the highest concentration (.01 uCi/L = 20 mg/L) were counted together. The organs were removed in 4 distinct catagories: Brain, skeletal system and skull, liver and heart, and intestines. The

groups were weighed and counted using the LSC and the converted mass of U absorbed was averaged over the 5 organ samples' mass and compared to that of the average U absorbed per total mass of those exposed to the same concentration. This method gave us a relative distribution of the DU and allowed theoritical calculations of the absorbed dose rate for each organ with the assumption that all energies were depostied locally in the organ.

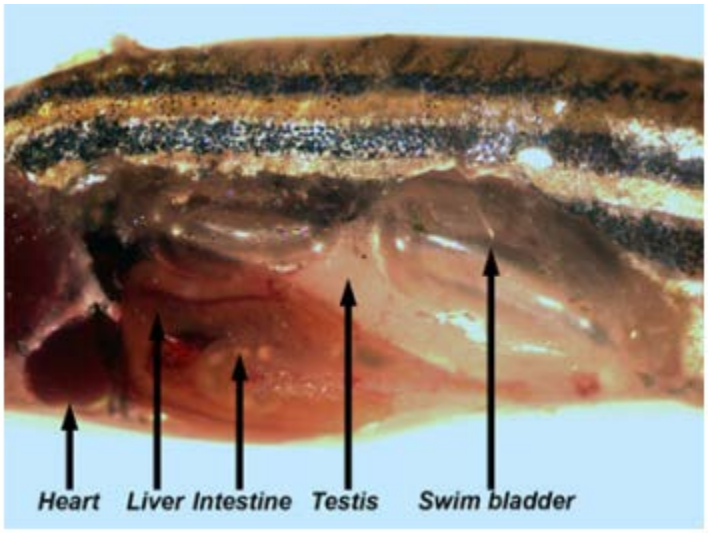

Figure 11 Zebrafish organ cross section (Gupta and Mullins 2010)

CHAPTER 3. RESULTS

3.1 Development Curve for Liquid Scintillation

From the figures below, Figure 12 shows the spectrum of a sample with no uranyl nitrate while Figure 13 shows a sample with uranyl nitrate dissolved in solution. We do see the peak in the 100 to 500 keV range from the alpha interactions, but more importantly, a lot of those energies were forced to the left due to the quenching effects. This means that any increase in counts, even below 100 keV, was contributed by the uranium decay, so instead of using the narrow window, the entire spectrum was taken into account when correlating counts to mass. As long as the counts increased fairly linearly with the increased mass of source, then we could create a standard curve relating mass to CPM. A few samples were also counted with small amounts of uranyl nitrate dissolved directly in the vial: 5, 15, and 25mg.

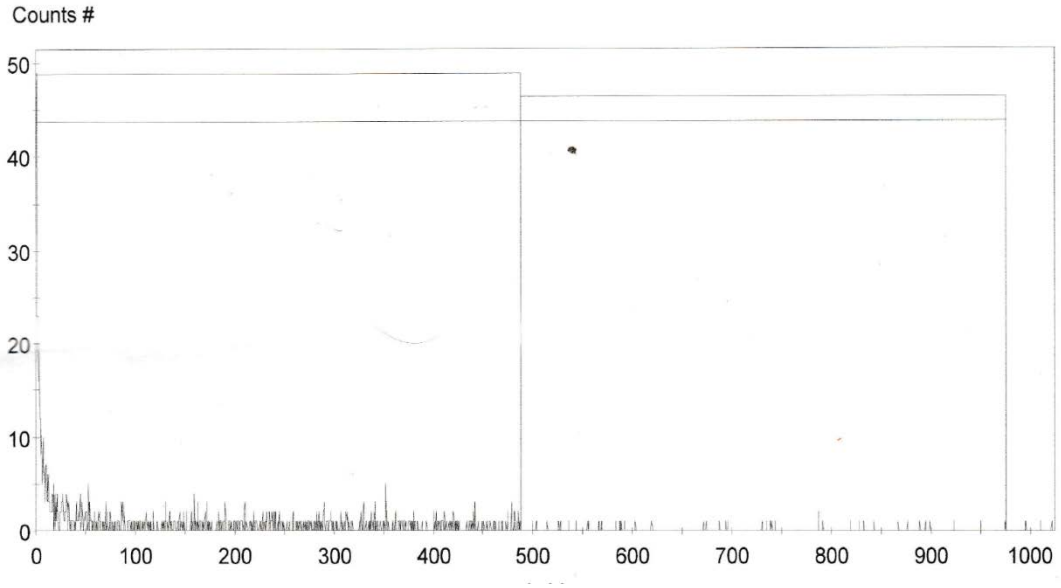

Figure 12 Perkin Elmer TriCarb 2800 Background Spectrum

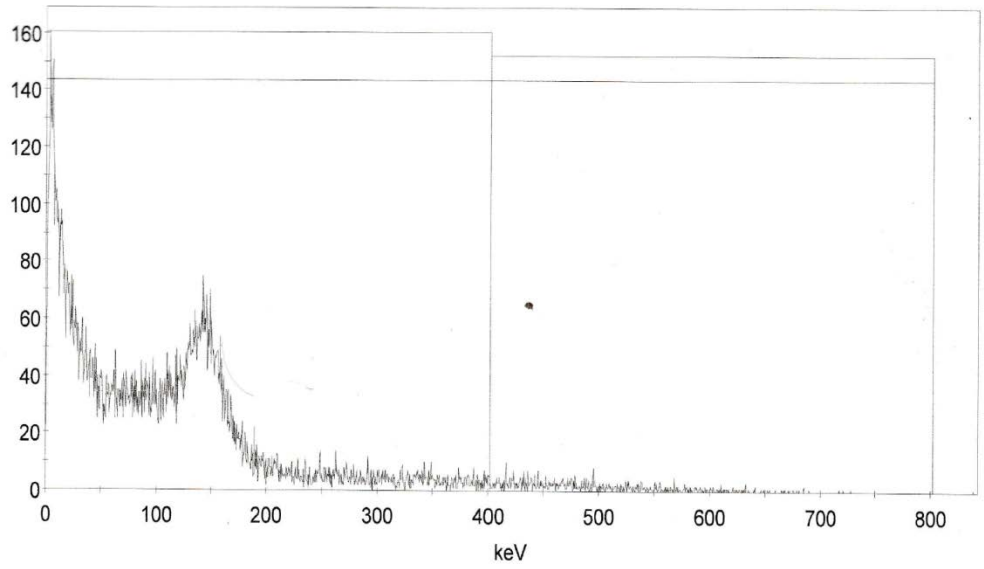

Figure 13 Perkin Elmer TriCarb 2800 Uranyl Nitrate Spectrum

Because the uranyl nitrate solution used exists in the form of $N_2O_8U{\bullet}6H_2O$, when dissolved in water, uranium makes up 60.408% of the mass and the counts recorded on the LSC were related to the mass of uranium. Table 1 shows the counts measured for the

different volume and mass of uranium with different samples, with each sample counted 3 times and the averages listed below.

Table 1 Mass Standards for LSC

Volume Added (mL)	Concentration Added (uCi/L)	Mass of Uranyl Nitrate (mg)	Mass of Uranium (mg)	Counts per Minute
1	0.001	0.003333	0.002014	0
2	0.001	0.006667	0.004027	2
3	0.001	0.01	0.006041	1
1	0.005	0.016667	0.010068	2
2	0.005	0.033333	0.020136	14
3	0.005	0.05	0.030204	30
1	0.015	0.05	0.030204	45
2	0.01	0.066667	0.040272	60
1	0.02	0.066667	0.040272	61
3	0.01	0.1	0.060408	64
2	0.015	0.1	0.060408	84
2	0.02	0.133333	0.080544	127
3	0.015	0.15	0.090612	136
3	0.02	0.2	0.120816	181
1	0.5	1.666667	1.0068	1345
2	0.5	3.333333	2.0136	2758
1	1	3.333333	2.0136	2887
0	0	5	3.0204	5099
3	0.5	5	3.0204	4896
2	1	6.666667	4.0272	5535
1	2.1	7	4.22856	6161
1	2.1	7	4.22856	6029
1	2.1	7	4.22856	6040
1	2.1	7	4.22856	6287
1	2.1	7	4.22856	6173

Table 1 Mass Standards for LSC (continued)

Volume Added (mL)	Concentration Added (uCi/L)	Mass of Uranyl Nitrate (mg)	Mass of Uranium (mg)	Counts per Minute
3	1	10	6.0408	8399
2	2.1	14	8.45712	12683
2	2.1	14	8.45712	12578
2	2.1	14	8.45712	12335
2	2.1	14	8.45712	12528
2	2.1	14	8.45712	12970
0	0	15	9.0612	14669
3	2.1	21	12.68568	18753
3	2.1	21	12.68568	18380
3	2.1	21	12.68568	18624
3	2.1	21	12.68568	18975
3	2.1	21	12.68568	18380
0	0	25	15.102	25169

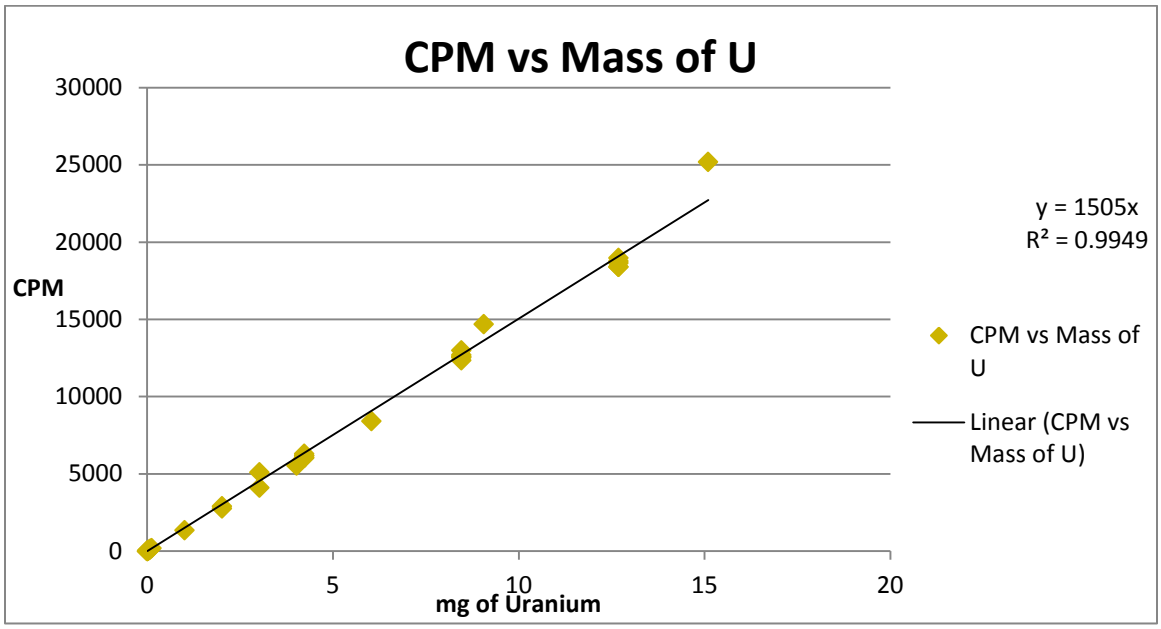

Figure 14 LSC CPM versus Mass of Uranium

From Table 1 and Figure 14 above, it can be concluded that the different volumes of water containing the different concentrations had little effect on the total counts seen by the LSC, with the exception of 0.001 uC/L, where the mass was so low, the activity observed was possible within the uncertainty of the detector. Plotting the total CPM versus the mg of uranium added gives us a fairly linear line. This allows us to establish a conversion of mg of uranium to CPM using the equation of the fitted line. For example, every mg of uranium will give us 1505 CPM, therefore, 10 mg of dissolved uranium should equal 15050 CPM. According to our data, 9 mg of uranium resulted in 14669 CPM. Therefore, this method proves that small volume changes have little to no effect of the total counts seen by the LSC. Some of these samples include different masses of tissue which will be discussed in and explained with Table 2.

Next was to determine if the dissolved mass of the tissue had any effects on the count rate. Of course the added tissue will cause further quenching thus shifting our spectrum to the left but we needed to know if the counts were affected. The same concentration was used in each vial, 2.1 uCi/L, along with 3 different volumes and 3 different amounts of tissue. This would combine the effects of volume and tissue while keeping the concentration the same and allow us to see if the counts were affected by adding different amounts of tissue. As before, all vials were counted using 1 mL of Biosol, .15 mL of 30% hydrogen peroxide solution, and 10 mL of Bioscint scintillation fluid.

Table 2 Tissue Mass Standards

Mass of Tissue (mg)	Volume (mL)	Concentration Added (uCi/L)	Mass of Uranyl Nitrate (mg)	Mass of Uranium (mg)	Counts per Minute
0	1	2.1	7	4.22856	6029
75.5	1	2.1	7	4.22856	6040
113	1	2.1	7	4.22856	6287
191.6	1	2.1	7	4.22856	6173
0	2	2.1	14	8.45712	12578
74.7	2	2.1	14	8.45712	12970
122.8	2	2.1	14	8.45712	12335
187	2	2.1	14	8.45712	12528
0	3	2.1	21	12.68568	18380
50	3	2.1	21	12.68568	18624
90	3	2.1	21	12.68568	18975
186.8	3	2.1	21	12.68568	18380

The tissue used was from dead zebrafish to reduce the need for more fish to be euthanized. Each amount of tissue was dissolved at 50 °C in 1 mL of Biosol. When comparing the averaged results to those of just different volumes, we can see that the tissue mass had little to no effect on the total counts recorded. This proves that even though some coloration and tissue may cause quenching, it will have little effect on the total recorded counts giving us a reasonable way to relate counts seen on the LSC to mass absorbed in each fish or organ.

3.2 Standard Curves for Ludlum 3030p

Various volumes and concentrations were evaporated in 2 inch diameter planchets. Each sample was counted for 10 minutes five different times. The counts were then converted

to dpm and compared to the theoretical dpm determined from the previous calculations. All alpha counts were converted from cpm to dpm using the 35% efficiency value for Pu-239, since the two beta emitters are in equilibrium with each other, the count distributions should be equivalent, therefore, all beta counts were divided by two and the proper efficiencies of 15% and 34% were applied to account for the dpm contributions of both Th-234 and Pa-234m.

Table 3 Alpha/Beta counts of Evaporated Uranium Masses

Mass of Uranium (mg)	**Alpha CPM**	**Beta CPM**	**Beta CPM/2**
0.060406	7	11	5.5
0.090609	12	18	9
0.120812	14	24	12
1.20812	286	401	200.5
1.81218	301	584	292
2.013332	339	702	351
3.0203	451	698	349
4.027268	501	826	413
4.22842	612	901	450.5
6.0406	649	1674	837
8.45684	1154	2541	1270.5
12.0812	1742	3429	1714.5
12.68526	1896	3894	1947
19.93398	2368	5712	2856
24.1624	2851	7024	3512

Table 4 compares the actual DPM shown by the meter compares to a calculated theoretical DPM. For example, using the concentrations discussed, for 1 g of U in compound: U-238, contributing 84.7% of the activity, Th-234, and Pa-234 all contribue .2541 uCi/g in equilibrium while U-235 and U-234 contribute .0033 and .0426

uCi/g respectively. This gives an actual total uCi/g of .8082 of compound. Calculating the relative DPM for each and summing them gives us a total theoritical DPM.

Table 4 Calculated DPM compared to theoretical DPM

Mass of Uranium (mg)	**Alpha DPM at 35%**	**Beta DPM at 15%**	**Beta DPM at 34%**	**Total DPM**	**Theoretical DPM**
0.060406	20	36.66667	16.17647	72.84314	108.38
0.090609	34.28571	60	26.47059	120.7563	162.57
0.120812	40	80	35.29412	155.2941	216.76
1.20812	817.1429	1336.667	589.7059	2743.515	2167.60
1.81218	860	1946.667	858.8235	3665.49	3251.41
2.013332	968.5714	2340	1032.353	4340.924	3612.32
3.0203	1288.571	2326.667	1026.471	4641.709	5419.02
4.027268	1431.429	2753.333	1214.706	5399.468	7225.72
4.22842	1748.571	3003.333	1325	6076.905	7586.63
6.0406	1854.286	5580	2461.765	9896.05	10838.04
8.45684	3297.143	8470	3736.765	15503.91	15173.26
12.0812	4977.143	11430	5042.647	21449.79	21676.09
12.68526	5417.143	12980	5726.471	24123.61	22759.89
19.93398	6765.714	19040	8400	34205.71	35765.55
24.1624	8145.714	23413.33	10329.41	41888.46	43352.18

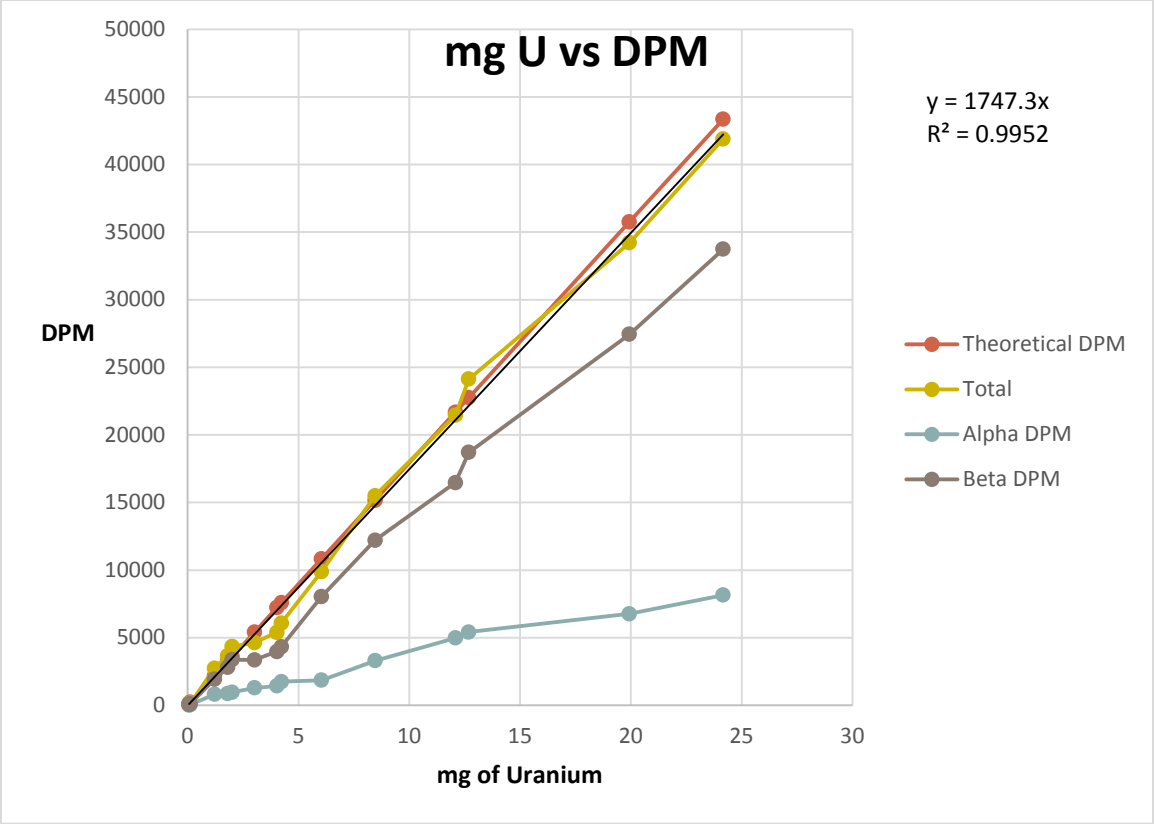

Figure 15 Graph of mg of U versus DPM on Ludlum 3030p

From the figure above, you can see that the total activity using the methods discussed is fairly close to the theoritical activity, 1747.3 dpm/mg vs 1794.204 dpm/mg, the variation is to be expected given an average of .3 uCi/g. Also, alpha counts seem to be lower than calculated at higher masses and this is probably due to the fact that more of the uranyl nitrate salt is needed to achieve the mass of uranium being measured; therefore, attenuation of the alpha particles through the salt increases. Of course it is very likely that the concentrations of each isotope may differ from the averages used in this calculation, but it appears the values are close enough for the purpose of this report.

Now we can compare expected alpha and beta DPM per isotope based on our assumptions discussed previously. This will allow to use the LSC to achieve total counts, which can then be converted to a mass of Uranium consumed, we can then relate the mass to calculate an approximately activity contribution from each isotope.

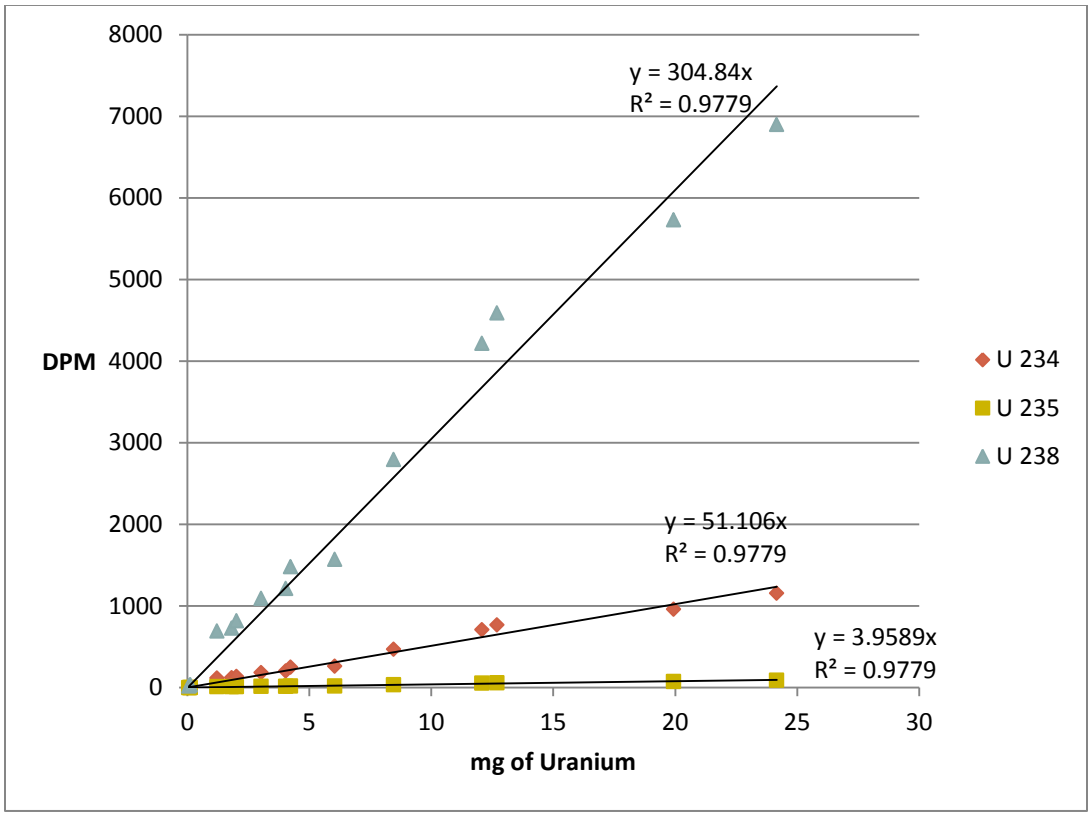

Figure 16 DPM contribution from each Uranium isotope

From Figure 16 we see that the contributions of each isotope are fairly linear, therefore, with a given mass of DU, we can correlate the mass of U to that of the activity contribution of each alpha emitting isotope.

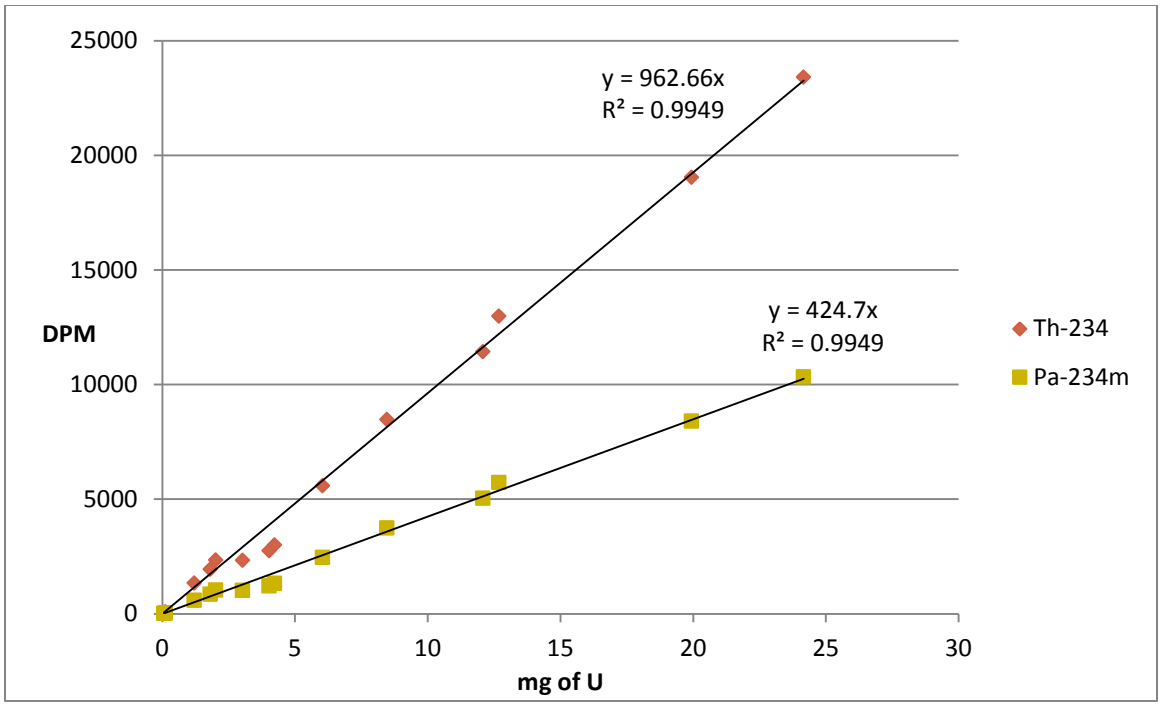

Figure 17 DPM contribution from Beta emitting isotopes

The same linear relationship exists for the beta emitters and will be used to convert the mass of DU to activity contributions from both Th-234 and Pa-234m.

3.3 Larvae Dose Distribution

3.3.1 Larva Bioconcentration Factor

As mentioned in chapter 2, only the counts from the second group of larvae were measured. Because it was shown that the larvae seemed more tolerant to the uranium added to each tank, higher concentrations of .005, .01, and .02 uCi/L were used. Table 5 and Table 6 reflect the results. Since the specific activity (SA) of the source was an average across the batch, that SA was used to calculate mass of U over mass of water. The mass concentration of U added to each was 10 mg/kg, 20 mg/kg, and 40 mg/kg,

which is 60.408% of the mass of uranyl nitrate dissolved. The results were averaged over the total number of fish alive after the dose period as each individual larva would be difficult to measure.

Table 5 Bioconcentration Factors for exposed larvae

# Exposed	Concentration of U Added (mg/kg)	# Alive after 7 days	Avg Mass per fish (mg)	Mass of U Absorbed per fish ug)	BCF
50(control)	0	46	0.289130435	0	0
50	10	47	0.229787234	0.169647275	73.33
50	20	45	0.335555556	0.472499077	69.93
50	40	44	0.329545455	0.936273029	70.55

Table 5 shows that the bioconcentration factor (BCF) is fairly consistent across the mass concentrations. This is probably due to the fact that the counts seen on the LSC and the mass of each larva were averaged over the number of fish alive after the 7 day exposure period. The BCF was calculated using the ratio of the mass concentration of U in fish to the mass concentration of U in the water.

3.3.2 Relative Absorbed Dose

Due to the size of the larva, we are assuming the mass of U is equally distributed throughout the entire body of each batch counted. There is no way to properly dissect the organs from the larva but due to the close proximity and size of the organism and the low amount of emitted particles, we can assume all absorbed energies are distributed homogeneously throughout the entirety of the organism

Table 6 Absorbed Dose Rate from Absorbed U

Concentration of U added (mg/kg)	**Mass of U Absorbed per fish (ug)**	**Dose Rate for U-234 (Gy/s)**	**Dose Rate for U-235 (Gy/s)**	**Dose Rate for U-238 (Gy/s)**	**Dose Rate for Th-234 (Gy/s)**	**Dose Rate for Pa-234m (Gy/s)**	**Total Dose Rate (mGy/d)**
0	0	0	0	0	0	0	**0**
10	0.1696	4.89E-10	1.71E-09	2.52E-09	3.03E-10	1.91E-09	**0.5998**
20	0.4725	1.36E-09	4.56E-09	7.02E-09	8.43E-10	5.33E-09	**1.1320**
40	0.9363	2.71E-09	8.85E-09	1.39E-08	1.67E-09	1.06E-08	**2.2719**

3.4 Adult Fish Dose Distribution

3.4.1 Bioconcentration Factor for Adult Fish

Table 7 shows the results of the BCFs for adult fish. Similar to other studies performed for bioconcentration factor of U in zebrafish (Barillet, Palluel, Porcher, and Devaux 2010), the BCF seems to increase as the mass concentration of U is lowered.

Table 7 BCF for Adult Zebrafish

U Dissolved in water (mg/L)	Mass of Fish (mg)	U Absorbed in Fish (mg)	BCF	Average BCF	Standard Error (n=8)
20	71.3	0.3249	227.85	**130.60**	**16.52**
20	214	0.4379	102.31		
20	280	0.3967	70.84		
20	115	0.2651	115.27		
20	108.3	0.3236	149.39		
20	62.5	0.1714	137.14		
20	206	0.4246	103.05		
20	104.5	0.2904	138.93		
10	121	0.2299	190.00	**202.64**	**13.14**
10	158	0.2930	185.46		
10	130.4	0.1987	152.36		
10	51	0.1435	281.41		
10	145	0.3010	207.58		
10	154.4	0.3369	218.18		
10	147	0.2777	188.94		
10	91	0.1794	197.15		
2	98.5	0.2073	1052.33	**774.72**	**273.90**
2	115	0.1435	624.01		
2	165.3	0.1794	542.66		
2	75.2	0.1661	1104.47		
2	89.8	0.2060	1146.88		
2	107.6	0.1402	651.48		
2	200	0.1429	357.14		
2	121.1	0.1741	718.77		
0	202	0	0		
0	147.3	0	0		
0	89.4	0	0		
0	92	0	0		
0	115.2	0	0		
0	79.8	0	0		
0	184.5	0	0		
0	215	0	0		

It's important to note that 20 ppm U was the highest concentration that guaranteed survival over the 7 day exposure period. Fish dosed to 60 ppm died within 3 hours, those exposed to 40 ppm died between 3 and 8 hours, and 30 ppm resulted in death between 8 and 16 hours. All water parameters (pH, conductivity, etc.) were relatively constant between these three concentrations which points to the fact that the toxicity level of U at some point just above 20ppm will cause lethality.

3.4.2 Dose Distribution for Adult Fish

The organs were dissected from 5 of the highest exposed fish and grouped into 4 categories: blood containing organs (heart, liver), brain, intestines, and skeletal system to include parts of the skull. Table 8 shows the percent of the averaged total absorbed U per organ averaged over the 5. The percent U per organ was calculated using the average mass of U absorbed per organ mass to that of the average mass concentration of the entire fish exposed to 20 mg/L of U. It is important to note that the kidneys, muscle and fat, and remainder of the fish could not be isolated for counting.

Table 8 U distribution per organ at 20 mg/L

Organ System	Average Mass per Organ (mg)	Mass of U Dissolved (mg/L)	Mass of U Absorbed per Organ (ug)	Percent U Mass Concentration per Organ
Blood Organs	1.50	20	5.4485	**13.8941**
Brain	1.66	20	1.5947	**3.6746**
Intestines	1.30	20	3.0565	**8.9934**
Skeletal System	2.24	20	12.6246	**21.5583**

Table 9 Absorbed Dose Rate due to absorbed U

Organ Group	Mass of U absorbed (ug)	Dose Rate for U-234 (Gy/s)	Dose Rate for U-235 (Gy/s)	Dose Rate for U-238 (Gy/s)	Dose Rate for Th-234 (Gy/s)	Dose Rate for Pa-234m (Gy/s)	Total Dose Rate per Organ (mGy/d)
Blood Organs	5.4485	2.41E-06	1.80E-07	1.24E-05	1.49E-06	9.42E-06	**2.2382**
Brain	1.5947	6.37E-07	4.74E-08	3.28E-06	3.95E-07	2.49E-06	**0.5919**
Intestines	3.0565	1.56E-06	1.16E-07	8.03E-06	9.67E-07	6.10E-06	**1.4487**
Skeletal System	12.6246	3.74E-06	2.78E-07	1.92E-05	2.32E-06	1.46E-05	**3.4728**

The percentages of U mass found in the organs compared to that of the mass of the entire fish as a whole seem consistent with those found in humans (HPS Fact Sheet 2012). The skeletal system seems to concentrate more of the U than the other organs while the brain concentrates the least. There may be variation in the intestines as fluctuations in counts may occur depending on when the fish eats and how long the food has been sitting in solution.

CHAPTER 4. DISCUSSION

It is known that LSC counting techniques usually result in nearly 100% efficiency when counting for alpha activity. Our samples consisted of both alpha and beta activity and due to quenching, the energy observed were observed at lower energy levels. This may have caused some loss in counts which can account for the difference in CPM per mass of the LSC versus calculated DPM per mass of the Ludlum 3030p. Also, due to the nature of the production of DU, our source most likely did not have a standard activity associated with it. All calculations of masses added to solutions were based off the manufacturer's information that the batch our uranyl nitrate came from had an average specific activity of 0.3 uCi/g.

Pairing the two instruments would seem to solidify the activity per unit mass in each sample. Though statistical analysis will prove to provide rather large variations of counts when going from CPM to mass, followed by mass to DPM, the trends were fairly linear and consistent. These discrepancies would only affect the calculated activity per fish or per organ which would create errors in the dose rate calculations but due to the low activity of DU, it requires very large concentrations for a formidable dose to be seen.

Due to consistency in the counts versus the mass used throughout the standards, it is clear that the Perkin Elmer TriCarb 2800 can be used to quantify total counts versus mass of U beginning at very low levels. This alone was beneficial enough to determine

the distribution of the U in the organs when compared to the distribution in fish of different masses. Organ specific distributions of 21.6% was found for bone, 13.9% for blood containing organs, 9% for intestines, and 3.7% for the brain which could possibly have skull fragments included. These distributions are similar in hierarchy to those found in humans exposed to DU. According to the HPS Human Health Fact Sheet from ANL, October 2001, 22% of the ingested uranium that finds its way to the blood stream is deposited into the bone while 12% is deposited into the kidneys (HPS ANL 2001). If we assume all of our uranium was ingested, outside of the amount finding its way to the intestines, the distribution is very similar.

Although some error can occur due to the each organ resulting in such low mass and the activity, it would be difficult to measure the distribution individually, at least not at 3 mpf. Fully mature zebrafish would allow easier dissection and separation of the organs and my limit mixing of the organ tissue if tearing occurs or loss of pieces of the skull when the brain is removed. A higher active source with a known activity level and allowing the fish to fully mature would allow easier counting and tracking of the source while minimizing the amount needed to be added, and permitting easier to access to specific organs with less cross contamination.

Calculated absorbed dose rate was calculated for the observed organs based on the mass of U detected by the LSC and converted to activity using the Ludlum 3030p. The activity per unit mass of each organ was used along with the specific energies of each radioactive decay and the highest dose rate was found to be in the skeletal system at 3.47 mGy/d which corresponds to it having the highest mass concentration of uranium and being consistent with studies showing that uranium finding its way to the bone structure.

The BCF was also shown to go up as the mass concentration was lowered in each environment. This is consistent with similar studies performed where much smaller concentrations were used. In a similar study, it was shown that for exposures to concentrations of 20 ug/L, 100 ug/L, and 500 ug/L, the average BCFs after 20 days were 1033.3, 359.5, and 92.8 respectively (Barillet, Palluel, Porcher, and Devaux 2010). This trend is solidified in these results with BCFs of 130.6 ± 16.5, 202.6 ± 13.14, and 774.7 ± 273.9 for concentrations of 20 mg/L, 10 mg/L, and 2 mg/L. The BCFs could not be directly compared as any small changes in the percentages of mass measured in mg to that of ug produces a significant difference in the mass concentrations when relating to the Barrillet experiment.

It was surprising how much more tolerant the larvae was when compared to that of the 3 mpf adults. The first exposure concentrations of 0.1, 0.5, and 1 uCi/L showed normal survival up to 0.1 uCi/l. For the adults, any exposure over 0.01 uCi/L resulted in death within a day, with the concentration of 0.015 uCi/L having the longest survival of approximately 8 to 16 hours. This shows that the adult zebrafish are very susceptible to the heavy metal toxicity of DU when exposed to concentrations over 20 ppm. It was surprising that the difference between 20 ppm and 30 ppm resulted in such a large difference in survival, 100% to 0% in a couple of hours, longer exposure studies should be performed to solidify the concentration that is lethal as 20 ppm could have resulting in lethality at any amount of time past 7 days.

This study shows that there are multiple methods of tracking exposure and distribution of DU in zebrafish. Using the natural decay emissions allowed tracking of the isotope as it concentrated in different parts of the body. This method, along with exposure

to other metals such a lead, can contribute to ongoing studies of combined exposures to natural environmental hazards. More importantly, with the zebrafish model, long term studies using other isotopes, such as Radium 223, combined with lead exposures, can provide principal information on the long term effects of alpha radiation combined with other toxic metals, specifically behavioral and genetic changes later in life.

CHAPTER 5. CONCLUSION

Detailed measurements of absorbed U in zebrafish have been studied. This method shows that the LSC is capable of determining a linear relationship between mass absorbed versus counts registered and paired with the Ludlum 3030p, a distinction can be made on the activity deposited. The distribution of U in zebrafish is similar to that of humans with a majority of the concentration seeking out the bone structure and the blood filtering organs.

Also, it was found that the larva were much more tolerant, almost by a factor of 10, to U exposure. There was some survival at concentrations upwards of 100 ppm while the adults had zero survival in excess of 20 ppm. Although, the BCFs were consistent at all concentrations found in the larvae, the BCF for the adults proved increase as the mass concentration of U decreased. This trend has been proven before in similar studies and leads to the conclusion that, depending on the mass of the fish, there is some equilibrium that is achieved as far as accumulation of U is concerned

BIBLIOGRAPHY

BIBLIOGRAPHY

Alamelu, D. and S. K. Aggarwal. "Determination of 235u/238u Atom Ratio in Uranium Samples Using Liquid Scintillation Counting (Lsc)." Talanta 77, no. 3 (Jan 15 2009): 991-4.

Alpen EL. Radiation Biophysics. (2nd Edition). New York: Academic Press; 1998.

American Veterinary Medical Association “Guidelines for the Euthanasia of Animals” 2013 Edition.

Attix FH. Introduction to Radiological Physics and Radiation Dosimetry. New York: John Wiley & Sons; 1986.

Barillet, S., Adam-Guillermin, C., Palluel, O., Porcher, J., and Devaux, A. (2010) “Uranium bioaccumulation and biological disorders induced in zebrafish (Danio rerio) after depleted uranium waterborne exposure” Environ Pollut, Vol. 159(405-502).

Bark W.,and Berger M.,Tables of Energy Losses and Ranges of Heavy Charged Particles, NASA-SP-3013(1964).

Bergonié J and Tribondeau L. De quelques résultats de la radiotherapie et essai de fixation d'une technique rationnelle. Comptes-Rendus des Séances de l'Académie des Sciences 143: 983–985; 1906.

Bergonié J and Tribondeau L. De quelques résultats de la radiotherapie et essai de fixation d'une technique rationnelle. Comptes-Rendus des Séances de l'Académie des Sciences 143: 983–985; 1906.

Bichsel H., Groom D., and Klein S., Passage of Particles through Matter, 2007; 11:19.

Bleise A., Danesi P., Burkart W., “Properties, Use, and Health Effects of Depleted Uranium (DU)” Austria: IAEA; 2002.

Bower K., Angel A., Gibson R., Robinson T., Knobeloch D., Smith B., “Alpha-beta Discrimination Liquid Scintillation Counting for Uranium and its Daughters” Journal of Radioanalytical and Nuclear Chemistry: 1994; Vol 181, p. 97-107.
.

Brennan, C. Why Zebrafish Make Excellent Research Models, National Centre for the Replacement of Refinement & Reduction of Animals in Research; 2014.

Cember, H. and T. E. Johnson (2009). Introduction to health physics. New York, McGraw-Hill Medical.

D'Costa, A. and I. T. Shepherd (2009). "Zebrafish development and genetics: introducing undergraduates to developmental biology and genetics in a large introductory laboratory class." Zebrafish **6**(2): 169-177.

Fathi, R. A.; Matti, L. Y.; Al-Salih, H. S.; Godbold, D. (2013). "Environmental pollution by depleted uranium in Iraq with special reference to Mosul and possible effects on cancer and birth defect rates". Medicine, Conflict and Survival 29 (1): 7–25.

Garcia, J. F. and A. Tarancon. "Liquid Scintillation Spectrometry: A Technique with Future." Appl Radiat Isot 93 (Nov 2014): 1-6.

Gardner, D. G. and W. W. Meinke. "Beta-Ray Spectroscopy Using a Hollow Plastic Scintillator." Int J Appl Radiat Isot 3, no. 3 (Aug 1958): 232-9.

Gove N., M.J. Martin, Log-f tables for beta decay, Nucl. Data Tables A, 10 (1971), pp. 205–219.

Grimeland, B. "Absolute Counting of Beta-Particles by Means of a Plastic Scintillator." Int J Appl Radiat Isot 4, no. 1-2 (Dec 1958): 116-8.

Gupta, T., Mullins, M. C. Dissection of Organs from the Adult Zebrafish. J. Vis. Exp. (37), e1717, doi:10.3791/1717 (2010).

Hall EJ and Giaccia AJ.Radiobiology for the Radiologist (7th Edition). Philadelphia: Lippincott Williams & Wilson; 2012.

Hanahan D and Weinberg RA. The hallmarks of cancer. Cell 100: 57-70; 2000.

Health Physics Society Fact Sheet, ANL October 2001.

Hughesdon P., Two uses of uranyl nitrate. Royal Microscopical Society (Great Britain), J R Microsc Soc, 1949, Vol.69 (Pt. 1), p.1

[IAEA1989] In Situ Leaching of Uranium: Technical, Environmental and Economic Aspects , IAEA-TECDOC-492, IAEA Vienna 1989, 172 p.

International Commission on Radiological Protection. Age-Dependent Doses to Members of the Public from Intake of Radionuclides Reference Values. Oxford: Pergamon Press; ICRP Publication 69; Ann. ICRP 25 (1);1995.

International Commission on Radiological Protection. Age-Dependent Doses to Members of the Public from Intake of Radionuclides Part 5Reference Values. Oxford: Pergamon Press; ICRP Publication 72; Ann. ICRP 26 (1);1995.

International Commission on Radiological Protection. Basic Anatomical and Physiological Data for Use in Radiological Protection Reference Values. Oxford: Pergamon Press; ICRP Publication 89; Ann. ICRP 32 (3-4); 2002.

International Commission on Radiological Protection. Recommendations of the International Commission on Radiological Protection. Oxford: Pergamon Press; ICRP Publication 103; Ann. ICRP 37 (1–3); 2007.

Knoll GF. Radiation Detection and Measurement (4th Edition). United States: John Wiley & Sons; 2010.

Lamarsh L and Baratta A. Introduction to Nuclear Engineering (3rd Edition). New Jersey: Prentice Hall; 2001.

LEE S., KANG S., JANG D., LEE C., KANG S., KANG B., LEE W., KIM y., "Comparison of New Simple Methods in Fabricating ZnS(Ag) Scintillators for Detecting Alpha Particles", Nuclear Science and Technology: 2007; Vol/ 1, p. 194-197.

Malonda G., A. Grau Carles,"The ionization quench factor in liquid-scintillation counting standardizations" Appl. Radiat. Isot, 51 (1999), pp. 183–188.

Matthews M., B. Trevarrow, J. Matthews A virtual tour of the guide for zebrafish users, Lab. Anim., 31 (2002), pp. 34–40.

McDowell W. "Liquid Scintillation Alpha Counting and Spectrometry and its Application to Bone and Tissue Samples" Oak Ridge National Laboratory: 1982.
McDowell W. and McDowell B "Liquid Scintillation Alpha Spectrometry" Boca Raton: CRC Press.; 1994.

McDiarmid M., J.P. Keogh, F.J. Hooper, K. McPhaul, K. Squibb, R. Kane, R. DiPino, M. Kabat, B. Kaup, L. Anderson, Health effects of depleted uranium on exposed Gulf War veterans, Environ. Res., 82 (2000), pp. 168–180.

McDiarmid, Melissa A. (2001). "Depleted uranium and public health: Fifty years' study of occupational exposure provides little evidence of cancer". BMJ 322: 123–124.

Mould, Richard F. (2001). "Radiation dose from depleted uranium can now be measured". BMJ 322: 865–866.

National Diagnostics Laboratory, Mechanism for Liquid Scintillation Counting and Counting Efficiency and Quenching, 2012. <https://www.nationaldiagnostics.com/liquid-scintillation/articles>

Reed B and Jennings M 2010 Guidance on the Housing and Care of Zebrafish (Danio Rerio) (West Sussex, UK: RSPCA Research Animals Department).

Turner J., Atoms, Radiation, and Radiation Protection (3rd Edition), Weinheim: Wiley-VCH; 2007.

Wang, J. J. "A Quick Liquid Scintillation Counting Technique for Analysis of (9)(0)Sr in Environmental Samples." Appl Radiat Isot 81 (Nov 2013): 169-74.

Williamson, J. F., J. F. Dempsey, A. S. Kirov, J. I. Monroe, W. R. Binns, and H. Hedtjarn. "Plastic Scintillator Response to Low-Energy Photons." Phys Med Biol 44, no. 4 (Apr 1999): 857-7

Wilkins RC, Wilkinson D, Maharaj HP, Bellier PV, Cybulski MB, and McLean JRN. Differential apoptotic response to ionizing radiation in subpopulations of human white blood cells. Mutation Research 513: 27-36; 2001.

<www.wise-uranium.org > May 2016